

Spread of infectious disease through clustered populations

Joel C. Miller

December 15, 2008

Abstract

Networks of person-person contacts form the substrate along which infectious diseases spread. Most network-based studies of the spread focus on the impact of variations in degree (the number of contacts an individual has). However, other effects such as clustering, variations in infectiousness or susceptibility, or variations in closeness of contacts may play a significant role. We develop analytic techniques to predict how these effects alter the growth rate, probability, and size of epidemics and validate the predictions with a realistic social network. We find that (for given degree distribution and average transmissibility) clustering is the dominant factor controlling the growth rate, heterogeneity in infectiousness is the dominant factor controlling the probability of an epidemic, and heterogeneity in susceptibility is the dominant factor controlling the size of an epidemic. Edge weights (measuring closeness or duration of contacts) have impact only if correlations exist between different edges. Combined, these effects can play a minor role in reinforcing one another, with the impact of clustering largest when the population is maximally heterogeneous or if the closer contacts are also strongly clustered. Our most significant contribution is a systematic way to address clustering in infectious disease models, and our results have a number of implications for the design of interventions.

1 Introduction

Recently H5N1 avian influenza and SARS have raised the profile of emerging infectious diseases. Both can infect humans, but have a primary animal host. Typically such zoonotic diseases emerge periodically into the human population and disappear (*e.g.*, Ebola, Hanta Virus, and Rabies), but sometimes (*e.g.*, HIV) the disease achieves sustained person-to-person spread. With the advent of modern transportation networks, diseases that formerly emerged in isolated villages and died out without further spread may now spread worldwide.

A number of interventions are available to control emerging diseases, each with distinct costs and benefits. To design optimal policies, we must address several related, but nevertheless distinct, questions. How fast would an epidemic spread? How likely is a single introduced infection to result in an epidemic? How many people would an epidemic infect? We quantify these using \mathcal{R}_0 , the *basic reproductive ratio*, which measures the average number of new cases each infection causes early in the outbreak; \mathcal{P} , the probability that a single infection sparks an epidemic; and \mathcal{A} , the *attack rate* or fraction of the population infected in an epidemic. Understanding these different quantities and what affects them helps us to select policies with maximal impact for given cost.

Many different models are used to study disease spread. Perhaps the most important decision in developing a model is how the interactions of the population are represented. Because of the complexity of the population, it is invariably necessary to make simplifying assumptions. The errors (and therefore, the conclusions) resulting from many of these approximations are not well-quantified. In this paper we will focus on quantifying the impact of clustering (the tendency to interact in small groups) and individual-scale heterogeneity on the spread of an epidemic.

Based on how they handle clustering, models for population structure fit into a hierarchy of three classes (which in turn may be subdivided). At the simplest level the population is assumed to mix without any clustering. Most existing models fall into this category. At the most complex level, agent-based models are

used: the movements of each individual are tracked, and people who are in the same location are able to infect one another. These models typically require significant resources to develop, and the clustering is explicitly included. An intermediate level of complexity attempts to introduce the clustering as a parameter (or several parameters). Usually these models only consider clustering in terms of the number of triangles in a network, but as we shall see, other structures may play a role.

Before introducing the details of our model, we review some previous work. All the models we consider are Susceptible-Infected-Recovered (SIR) epidemic models [2], in which individuals begin susceptible, become infected by contacting infected individuals, and finally recover with immunity.

For unclustered populations, ordinary differential equation (ODE) models were among the earliest models used [24] and remain the most common. They are deterministic, and so cannot directly calculate \mathcal{P} , but they give insight into the factors controlling \mathcal{R}_0 and \mathcal{A} . Because they assume mass-action mixing, it is difficult to incorporate individual heterogeneity in the number of contacts. More recently some network-based models have been introduced for unclustered populations [3, 36, 23, 32, 29, 30, 31]. These models represent the population as nodes with edges between nodes representing contacts, along which disease spreads stochastically. Heterogeneity in the number of contacts is introduced by modifying the degree (number of edges) of each node. By neglecting clustering, these studies are able to make analytic predictions through branching process arguments. A recent sociological study [35] used surveys with participants recording the length and nature of their contacts. This data is valuable for providing the contact distribution needed for the above network models, and allows us to apply network results to real populations. However, this data does not directly tell us anything about the clustering of the population resulting from family/work/other groups. Other recent work by [32, 23] analytically addresses the impact of heterogeneity in infectiousness and susceptibility in unclustered networks.

Using agent-based simulations [15, 5, 11, 17, 19, 1] allows us to directly incorporate clustering. In these simulations, the population is a collection of individuals who move and contact one another. The modeller has complete control over the parameters governing interactions and how the disease spreads. This allows us to study many effects, but also introduces many parameters. It is difficult to test the accuracy of the assumptions used to generate these models and to extract which parameters are essential to the disease dynamics. The expense of developing these simulations is frequently prohibitive.

In this paper we introduce a systematic approach for calculating the impact of clustering, and quantifying the error. Because our model investigates disease spread in clustered networks, we provide a more detailed review of previous work on clustering and disease. A few investigations have been made into the interaction of clustering with disease spread using network models. The attempts that have been made [21, 14, 37, 40, 41, 8] typically use approximations whose errors are not quantified, resulting in apparently contradictory results. A few papers [33, 42, 25] have considered clustering and heterogeneities, rigorously showing that increased heterogeneity tends to decrease \mathcal{P} and \mathcal{A} , but without quantitative predictions. Recently [14] considered the spread of epidemics in a class of random networks for which the number of triangles could be controlled. It may be inferred from their figure 3 that clustering decreases the growth rate and that sufficient clustering can increase the epidemic threshold. However, at small and moderate levels clustering appears not to alter the final size of epidemics significantly. Similar observations have been made by [4]. At first glance, this contradicts observations of [40, 41] that clustering significantly reduces the size of epidemics, but that sufficiently strong clustering reduces the epidemic threshold (see also [37]), allowing epidemics at lower transmissibility. The discrepancy in epidemic size may be resolved by noting that the networks in [40, 41] have low average degree. We will see that clustering only affects the size if the typical degree is small or clustering is very high. The apparent discrepancy in epidemic threshold with strong clustering may be resolved by noting that the form of strong clustering considered by [40, 41] forces preferential contacts between high degree nodes. The reduction in epidemic threshold is perhaps better understood in terms of degree-degree correlations than in terms of clustering.

In this paper we develop techniques to incorporate general small-scale structure (beyond triangles) into the calculation of \mathcal{R}_0 , \mathcal{P} , and \mathcal{A} . To calculate \mathcal{R}_0 , we develop a systematic series expansion which allows us to interpolate between unclustered and clustered results by including more terms. To calculate \mathcal{P} and \mathcal{A} , we use a similar approach, but only give estimates on the size of correction terms. Our methods give us a

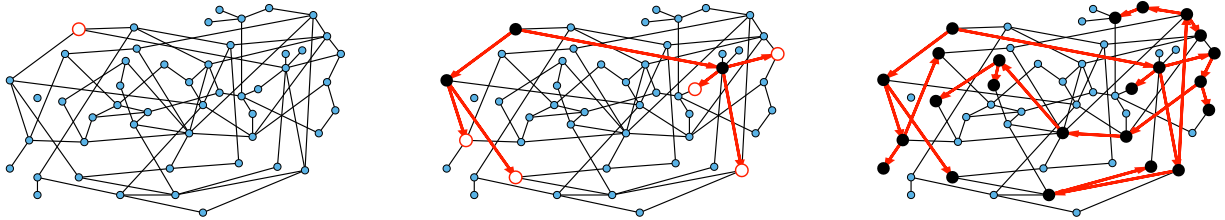


Figure 1: A sample network and several stages of an outbreak. Nodes begin susceptible (small circles), become infected (empty large circles), possibly infecting others along edges, and then recover (solid large circles). The outbreak finishes when no infected nodes remain.

rigorous means to understand how unclustered results relate to more realistic populations, and our results resolve the apparent discrepancies mentioned above. Our theory accurately predicts epidemic behaviour in a more realistic contact network derived from an agent-based simulation of Portland, Oregon by EpiSimS [11]. We expand this to investigate the interplay of clustering, heterogeneities in individual infectiousness or susceptibility, and variation in edge weights in their effect on \mathcal{R}_0 , \mathcal{P} , and \mathcal{A} .

The paper is organised as follows: Section 2 describes our model and networks and summarises earlier work on unclustered networks. These results will be the leading order terms for our expansions for clustered networks in the remainder of the paper. Section 3 considers how epidemics spread in a clustered network assuming homogeneous transmission. We derive the corrections to \mathcal{R}_0 and show that the corrections to \mathcal{P} and \mathcal{A} are insignificant unless the typical degree is small or clustering very high. Section 4 considers epidemics in clustered networks with heterogeneous infectiousness or susceptibility, building on section 3. Section 5 extends this further to consider epidemics spreading on clustered networks with weighted edges. Edges with large weights tend to occur in family or work groups which magnifies the impact of clustering. Finally section 6 discusses the implications of our results, particularly for designing interventions. We conclude that in general, heterogeneity significantly impacts \mathcal{P} and \mathcal{A} , but not \mathcal{R}_0 , while clustering impacts \mathcal{R}_0 significantly, but not \mathcal{P} and \mathcal{A} . Heterogeneity or edge weights may enhance the impact of clustering.

2 Formulation

2.1 The disease model

We consider the spread of a disease using a discrete SIR model on a static network G . Nodes of G represent individuals and edges represent (potentially infectious) contacts. The contact structure of the network is fixed during the course of the outbreak. The *degree* k of a node u is the number of edges containing u . Figure 1 shows a sample outbreak. A single infection, the *index case* is chosen uniformly from the population to begin an *outbreak*. Infection spreads along an edge from an infected node u to a susceptible node v with probability T_{uv} , the *transmissibility*. The time it takes for infection and recovery to occur may vary but does not affect our results. Once u recovers it cannot be reinfected. Typically for a large random network with a population of $N = |G|$ nodes, the final size of outbreaks is either large, with $\mathcal{O}(N)$ cumulative infections, or small, with $\mathcal{O}(\log N)$ infections [7]. Large outbreaks are *epidemics* and small outbreaks are *non-epidemic outbreaks*.

2.1.1 Transmissibility

A number of factors influence the transmissibility from u to v such as the viral load and duration of infection of u , the vaccination history and general health of v , the duration and nature of the contact between u and v , and characteristics of the disease.

For each node u we denote its ability to infect others by \mathcal{I}_u and its ability to be infected by \mathcal{S}_u . Each

edge has a weight w_{uv} . The parameter α measures disease-specific quantities. In most of our calculations we assume these are scalars and follow [32, 10], setting

$$T_{uv} = T(\mathcal{I}_u, \mathcal{S}_v, w_{uv}) = 1 - e^{-\alpha \mathcal{I}_u \mathcal{S}_v w_{uv}}. \quad (1)$$

If all contacts are identical, w_{uv} may be absorbed into α

$$T_{uv} = T(\mathcal{I}_u, \mathcal{S}_v) = 1 - e^{-\alpha \mathcal{I}_u \mathcal{S}_v}. \quad (2)$$

Note that T_{uv} is a number assigned to an edge, while $T(\mathcal{I}_u, \mathcal{S}_v)$ is a function which states what the transmissibility between two nodes would be if they shared an edge.

With mild abuse of notation we denote the probability density functions (pdfs) of \mathcal{I} , \mathcal{S} , and w by $P(\mathcal{I})$, $P(\mathcal{S})$, and $P(w)$ respectively. We assign \mathcal{I} and \mathcal{S} independently, but allow w to be assigned either independently or based on observed contacts (*i.e.*, by observing contacts in a population we may create a static network with edge weights assigned based on the observed contact). If w is assigned independently, then it is possible to eliminate edge weights from the analysis by marginalising over the distribution of weights. However, if weights are not independent (for example work or family contacts tend to have correlated weights) then the details of the distribution and the correlations are important.

Given the infectiousness \mathcal{I}_u of node u , we follow [32, 33] and define its *out-transmissibility*

$$T_{out}(u) = \iint T(\mathcal{I}_u, \mathcal{S}, w) P(\mathcal{S}) P(w) d\mathcal{S} dw. \quad (3)$$

This is the marginalised probability that u infects a randomly chosen neighbour given \mathcal{I}_u . From the definition of T_{out} and the pdf $P(\mathcal{I})$ we can calculate the pdf $Q_{out}(T_{out})$. We symmetrically define the *in-transmissibility* T_{in} and its pdf $Q_{in}(T_{in})$.

We denote the average of a quantity by $\langle \cdot \rangle$. The average transmissibility $\langle T \rangle$ is

$$\langle T \rangle = \iiint T(\mathcal{I}, \mathcal{S}, w) P(\mathcal{I}) P(\mathcal{S}) P(w) d\mathcal{I} d\mathcal{S} dw. \quad (4)$$

2.1.2 Epidemic percolation networks

Rather than studying outbreaks as dynamic processes on networks, we may consider them in the context of Epidemic Percolation Networks (EPNs) [22, 23, 33]. The EPN framework allows us to study epidemics as static objects and is useful for quickly estimating \mathcal{P} , \mathcal{A} , and \mathcal{R}_0 . In this section we summarise properties of EPNs; more details are provided in [22, 33, 32] and A.

Once the properties of the nodes and edges are assigned, an EPN \mathcal{E} is created as follows: We place each node of G into \mathcal{E} . For each edge $\{u, v\}$ in G we place directed edges (u, v) and (v, u) into \mathcal{E} independently with probability T_{uv} and T_{vu} respectively. The nodes infected in an outbreak correspond exactly to those nodes that may be reached from the index case following edges of \mathcal{E} . More specifically, the distribution of out-components of a node u in different EPN realisations matches the distribution of outbreaks resulting from different epidemic realisations in the original model with u as the index case. It may be shown that the distributions of out- and in-component sizes give us information about the probability of nodes to start an epidemic or become infected in an epidemic. We will see that in a large population the structure of a single EPN can be used to accurately estimate \mathcal{P} , \mathcal{A} , and \mathcal{R}_0 .

Once we create an EPN and choose the index case, we define the *rank* of node v as the length of the shortest directed path from the index case to v .¹ If no such path exists, v is never infected.

Interchanging all arrow directions interchanges \mathcal{P} and \mathcal{A} . This means that if we can calculate \mathcal{P} , then \mathcal{A} may be calculated by the same technique, but with the direction of infection reversed. Because of this, we focus our attention on calculating \mathcal{P} , and apply the same methodology to calculate \mathcal{A} . An important consequence is that if T is constant, then $\mathcal{P} = \mathcal{A}$ [36, 32].

¹We follow [26] in using the term *rank* rather than *generation* which has been used elsewhere, but is potentially ambiguous. The rank is the shortest number of infectious contacts between the index case and a node. It is possible that a different path takes less time. The path infection actually follows is the path that is shorter in time, rather than number of links.

2.1.3 The basic reproductive ratio

We expect that epidemics are possible if and only if the *basic reproductive ratio* \mathcal{R}_0 is greater than 1. That is, if an average infection causes more than one new case, an epidemic may occur, but otherwise the outbreak dies out quickly. However, this use of \mathcal{R}_0 is not consistent with the typical definition: *the average number of new infections caused by a single infected individual introduced into a fully susceptible population*, which gives $\mathcal{R}_0 = \langle T \rangle \langle k \rangle$. A more appropriate definition is *the average number of new infections caused by infected individuals early in outbreaks*. The distinction is subtle, but results from the fact that whether an outbreak can grow depends on whether the people of low rank infect more than one person each [12]. Low rank individuals may be different from the average individual. Most obviously, they have more contacts [36, 16]; but with clustering, they also have a disproportionately large fraction of neighbours infected or recovered.

In order to quantify \mathcal{R}_0 more rigorously, we first define N_r to be the number of people of rank r for a given outbreak simulation. We then define the *rank reproductive ratio*

$$\mathcal{R}_{0,r} = \frac{\mathbb{E}[N_{r+1}]}{\mathbb{E}[N_r]} \quad (5)$$

to be the expected number of new cases caused by a rank r node (averaged over all possible outbreak realisations). $\mathcal{R}_{0,0} = \langle T \rangle \langle k \rangle$ corresponds to the usual definition of \mathcal{R}_0 . In practise, we find that $\mathcal{R}_{0,r}$ reaches a plateau quickly as r increases before eventually decreasing as the finite size of the population becomes important. Consequently, an improved definition of \mathcal{R}_0 is the limit of $\mathcal{R}_{0,r}$ as r grows, subject to the assumption that $\mathcal{R}_{0,r}$ is unaffected by the finite size of G . This gives (cf, [42])

$$\mathcal{R}_0 = \lim_{r \rightarrow \infty} \lim_{|G| \rightarrow \infty} \mathcal{R}_{0,r} . \quad (6)$$

and generalises the definition given by [12] for ODE models. Under this definition, epidemics are possible if $\mathcal{R}_0 > 1$, but not if $\mathcal{R}_0 < 1$. We discuss this further in B. In a large population considering multiple index cases with a single EPN gives a good estimate of $\mathbb{E}[N_r]$ and hence $\mathcal{R}_{0,r}$.

2.2 Configuration Model Networks

We consider two different types of networks. The first is a class of (unclustered) random networks for which we can derive analytic results based only on the degree distribution. These analytic results will form the leading order term of our perturbation expansions. The second is a more complicated network resulting from an agent-based simulation, which we will use to demonstrate the accuracy of our perturbation expansions.

Our random networks are created by an algorithm which has been discovered independently a number of times (see *e.g.*, [34] and [6]). These have come to be called Configuration Model (CM) [38] networks. These networks are maximally random given the degree distribution. As the number of nodes in a CM network grows, the frequency of short cycles becomes negligible. The resulting lack of clustering allows us to calculate analytic results for epidemics. We briefly discuss these results assuming T is constant. More details are in [3, 36, 30, 23, 32, 39, 28] and C (which also addresses edge weights).

In the early stages of an outbreak in a CM network, the probability that a newly infected (non-index case) node has degree k is $kP(k)/\langle k \rangle$. Clustering is unimportant and so the node will have $k-1$ susceptible neighbours, regardless of its rank. Thus the expected number of infections caused by a newly infected node is

$$\mathcal{R}_0 = T \frac{\langle k^2 - k \rangle}{\langle k \rangle} . \quad (7)$$

To calculate the probability \mathcal{P} that infection of a randomly chosen index case results in an epidemic, we instead calculate the probability $f = 1 - \mathcal{P}$ that it does not. Then f is the probability that each neighbour of the index case either is not infected, or is infected but does not start an epidemic. Defining h to be the probability that a secondary case does not start an epidemic,

$$f = \sum_k P(k) [1 - T + Th]^k . \quad (8)$$

We find a similar relation for h , except that the probability for a secondary case to have degree k is $kP(k)/\langle k \rangle$ and only $k - 1$ neighbours are susceptible

$$h = \frac{1}{\langle k \rangle} \sum_k kP(k)[1 - T + Th]^{k-1}. \quad (9)$$

We solve this recurrence relation for h numerically, and use the result to find f . \mathcal{P} follows immediately. Because T is constant, this also gives \mathcal{A} [36, 32].

If T is not constant, the calculation becomes more difficult, and is discussed further in C and [23, 32]. In general, if T can vary for CM networks, $\mathcal{R}_0 = \langle T \rangle \langle k^2 - k \rangle / \langle k \rangle$, while \mathcal{P} and \mathcal{A} are overestimated by the values calculated assuming constant T .

2.3 The EpiSimS Network

We are interested in understanding the impact of clustering on disease spread. The term *clustering* is rather vague, and is usually measured by the number of triangles in a network [43]. However, any sufficiently short cycles impact the spread of an infectious disease. For our purposes we think of a clustered network as a network with enough short cycles to impact disease dynamics.

It is relatively simple to measure the degree distribution of a population using survey methods. We can easily calculate \mathcal{P} , \mathcal{A} , and \mathcal{R}_0 for a CM network with the same degree distribution, but the error between these values and the values for the original clustered network are unknown. Our goal in this paper is to develop analytical techniques to quantify these errors.

To test our predictions we turn to an agent-based network derived from a single EpiSimS [11, 15, 5] simulation of Portland, Oregon. The simulation includes roads, buildings, and a statistically accurate (based on Census data) population of approximately 1.6 million people who perform daily tasks based on population surveys. This gives a highly detailed knowledge of the interactions in the synthetic population. The degree distribution and contact structure emerge from the simulation. The resulting network has significant clustering and average degree of about 16. More details are in D.

3 Clustered networks with homogeneous nodes

In this section we assume that the population is homogeneous and all contacts are equally weighted. Consequently transmissibility is constant: $T_{uv} = T$ for all edges. It follows that $\mathcal{P} = \mathcal{A}$ [36, 32]. We develop a predictive theory for \mathcal{P} , \mathcal{A} , and \mathcal{R}_0 and test the theory with simulations on the EpiSimS network. We begin with \mathcal{R}_0 .

3.1 The basic reproductive ratio

The simulated rank reproductive ratio $\mathcal{R}_{0,r}$ is shown in figure 2 for $0 \leq r \leq 4$. At all values of T , $\mathcal{R}_{0,0} = T \langle k \rangle$ is clearly distinct from $\mathcal{R}_{0,r}$, $r > 0$ (which are close together). For $r > 0$, $\mathcal{R}_{0,r}$ is asymptotic to the unclustered approximation $T \langle k^2 - k \rangle / \langle k \rangle$ as $T \rightarrow 0$. This is because at small T the disease only rarely follows all edges of short cycles and so clustering has no impact. As T increases, these curves lie significantly below the unclustered approximation, because clustering reduces the number of available susceptibles. $\mathcal{R}_{0,4}$ peels away from $\mathcal{R}_{0,1}$, $\mathcal{R}_{0,2}$, and $\mathcal{R}_{0,3}$ for larger T because the population is finite, and so the number of susceptibles available to infect after rank four is reduced. In larger populations, $\mathcal{R}_{0,4}$ would not deviate.

We conclude that $\mathcal{R}_{0,r}$ converges quickly, and that $\mathcal{R}_{0,1}$ is a good approximation to \mathcal{R}_0 , but $\mathcal{R}_{0,0}$ is not. This implies that the network has important structure contained in paths of length 2, but not in paths of length 3. This fortunate observation allows us to approximate \mathcal{R}_0 by $\mathcal{R}_{0,1}$, which we may analytically calculate with relative ease ($\mathcal{R}_{0,r}$ becomes combinatorially hard as r grows). To find $\mathcal{R}_{0,1} = \mathbb{E}[N_2]/\mathbb{E}[N_1]$ we first note that $\mathbb{E}[N_1] = T \langle k \rangle$. Calculating $\mathbb{E}[N_2]$ is more difficult: consider all pairs of nodes u and v with at least one path of length 2 between them. Let n_{uv} be the number of paths of length 2 between u and v and χ_{uv} be an indicator function: $\chi_{uv} = 1$ if $\{u, v\}$ is an edge and $\chi_{uv} = 0$ if it is not (see figure 3). The

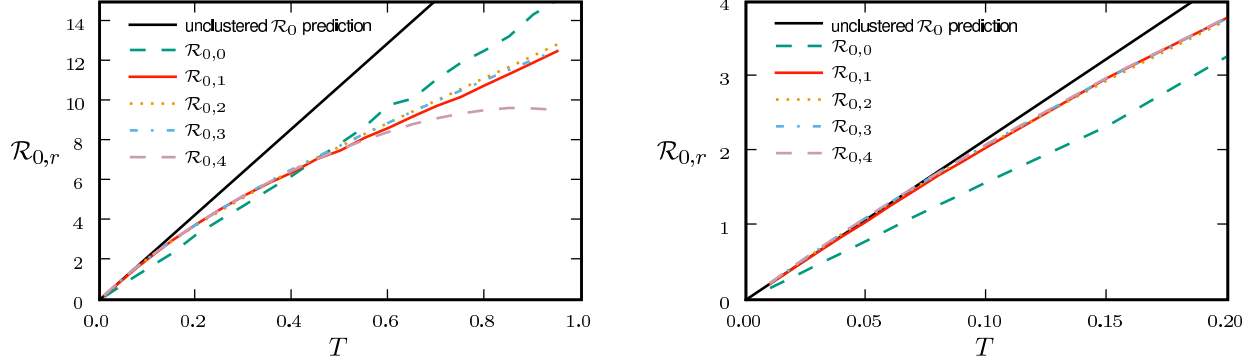


Figure 2: Simulated values of the rank reproductive ratio $\mathcal{R}_{0,r} = \mathbb{E}[N_{r+1}]/\mathbb{E}[N_r]$ for $r = 0, \dots, 4$ using an EPN from the (fixed) EpiSimS network with a homogeneous population, compared with the unclustered prediction. At small T (right panel) $\mathcal{R}_{0,1}-\mathcal{R}_{0,4}$ match the unclustered prediction.



Figure 3: Different options for paths of length two between nodes u and v .

probability that an infection of u results in infection of v in exactly two steps is $[1 - (1 - T^2)^{n_{uv}}][1 - T]^{\chi_{uv}}$. Summing this over all pairs yields

$$\mathbb{E}[N_2] = \frac{1}{N} \sum_u \sum_{v \neq u} [1 - (1 - T^2)^{n_{uv}}][1 - T]^{\chi_{uv}},$$

(where N is the size of the population and each pair u and v appears twice) which allows us to calculate $\mathcal{R}_{0,1}$ exactly. This sum is straightforward to calculate, but we can increase our understanding with a small T expansion. We approximate $\mathbb{E}[N_2]$ for $T \ll 1$ by

$$\begin{aligned} \mathbb{E}[N_2] &= \frac{1}{N} \sum_u \sum_{v \neq u} T^2 n_{uv} (1 - T)^{\chi_{uv}} - \binom{n_{uv}}{2} T^4 + \mathcal{O}(T^5), \\ &= T^2 \langle k^2 - k \rangle - 2T^3 \langle n_{\Delta} \rangle - T^4 \langle n_{\square} \rangle + \mathcal{O}(T^5), \end{aligned}$$

where $\langle n_{\Delta} \rangle = \frac{1}{N} \sum_u \sum_{v \neq u} n_{uv} \chi_{uv}$ is the average number of triangles each node is in, and $\langle n_{\square} \rangle = \frac{1}{N} \sum_u \sum_{v \neq u} \binom{n_{uv}}{2}$ is the average number of squares each node is in (*cf.*, [20]). Higher order terms involve more complicated shapes. This gives

$$\mathcal{R}_{0,1} = \frac{\langle k^2 - k \rangle}{\langle k \rangle} T - \frac{2 \langle n_{\Delta} \rangle}{\langle k \rangle} T^2 - \frac{\langle n_{\square} \rangle}{\langle k \rangle} T^3 + \mathcal{O}\left(\frac{T^4}{\langle k \rangle}\right). \quad (10)$$

At leading order we recover the unclustered prediction for \mathcal{R}_0 , reflecting the fact that at small T the probability the outbreak follows all edges of a cycle is negligible. As T increases, the first corrections are due to triangles, then squares, then pairs of triangles sharing an edge, and sequentially larger and larger

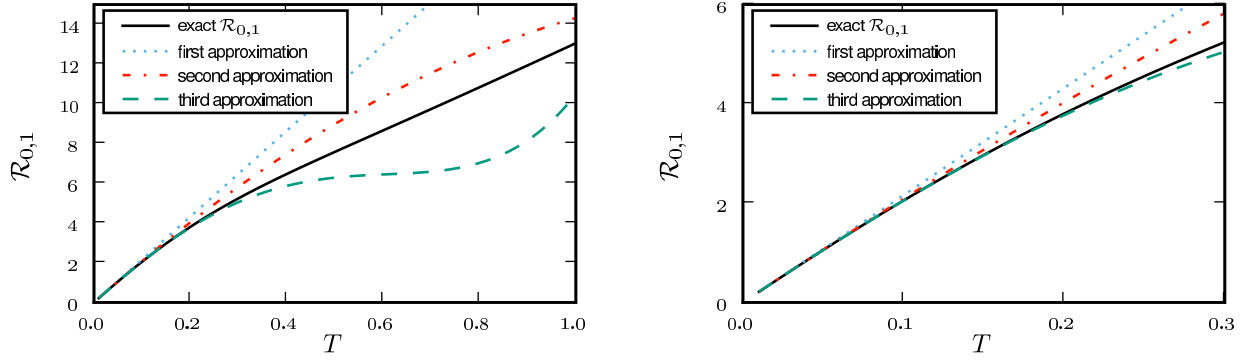


Figure 4: Comparison of first three asymptotic approximations for $\mathcal{R}_{0,1}$ from equation (10) with the exact value (solid) for the EpiSimS network. The right panel shows the comparison at small T .

structures made up of paths of length two. A comparison of these approximations with the exact value is shown in figure 4.

Although we have defined \mathcal{R}_0 for an ensemble of realisations, figure 5 shows that $\mathcal{R}_{0,1}$ accurately predicts the observed ratio N_{r+1}/N_r for individual simulations once the outbreaks are well-established. Early in outbreaks, the behaviour is dominated by stochastic effects, and so the ratio of successive rank sizes is noisy. Once the outbreak has grown large enough, random events become unimportant and the ratio settles at $\mathcal{R}_{0,1}$.²

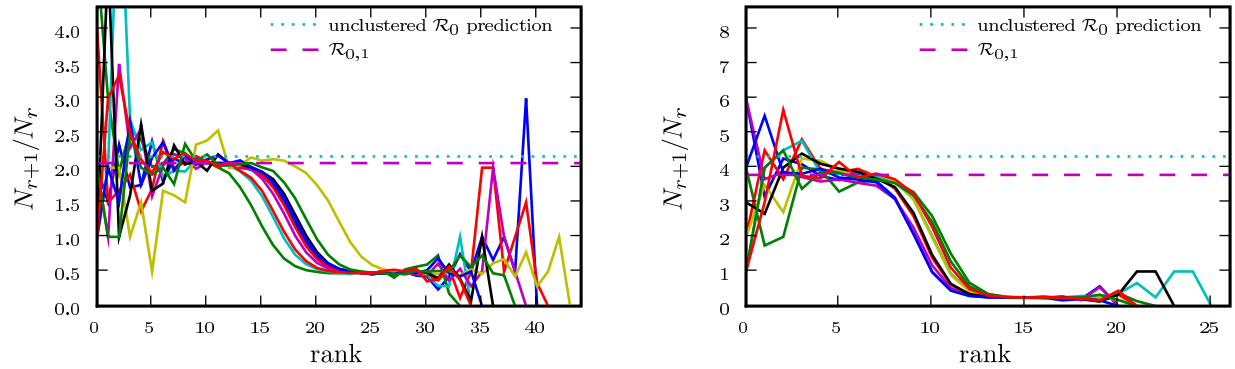


Figure 5: The progression of ten simulated epidemics for (left) $T = 0.1$ and (right) $T = 0.2$ in the EpiSimS network. The left panels show N_{r+1}/N_r against rank and right panels show the cumulative fraction of the population infected.

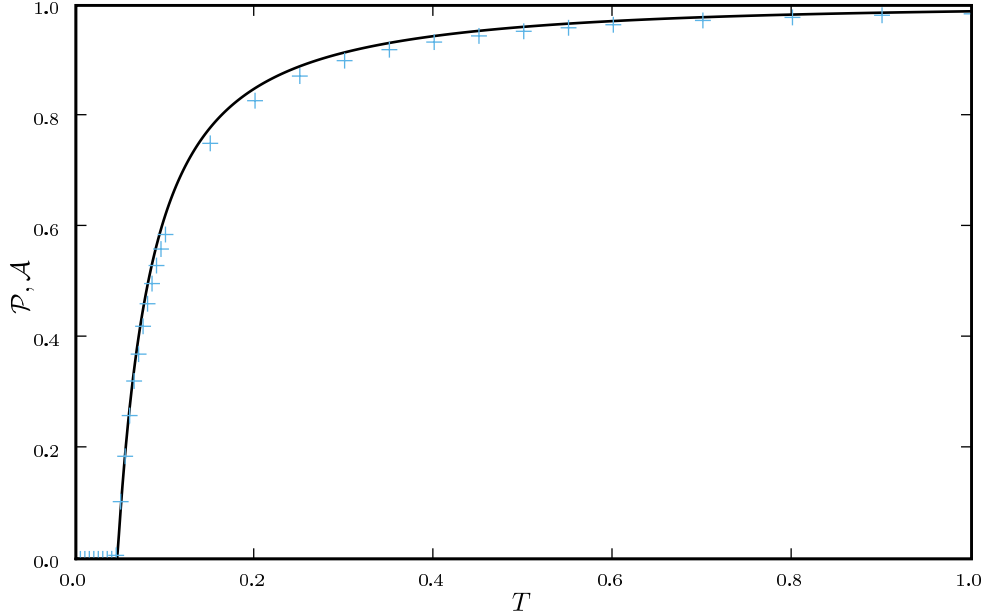


Figure 6: Probability \mathcal{P} and attack rate \mathcal{A} of epidemics for the (clustered) EpiSimS network (+) versus T , compared to the prediction derived from the degree distribution assuming no clustering. Each data point is from a single EPN, (the variation in \mathcal{P} resulting from different EPNs is negligible).

3.2 Epidemic probability and size

In order to assess the effect of clustering on \mathcal{P} and \mathcal{A} , we compare epidemics on the EpiSimS network with the analytic predictions derived assuming a CM network of the same degree distribution in figure 6. The epidemic threshold is not noticeably altered, and the values of \mathcal{P} and \mathcal{A} are almost indistinguishable from the predictions made assuming no clustering, despite the large amount of clustering in the network.

Although initially surprising, these results may be understood intuitively as follows: if T is large enough that the disease follows all edges of a short cycle then some other edge from a node of that cycle is likely to start an epidemic and the cycle does not prevent an epidemic. On the other hand, if T is smaller so that it does not follow all edges of a cycle, then the disease never sees the existence of the cycle, and the outbreak progresses as if there were no cycle.

To make this more rigorous, we first look at the epidemic threshold. We assume \mathcal{R}_0 is well-approximated by $\mathcal{R}_{0,1}$. Let $T_0 = \langle k \rangle / \langle k^2 - k \rangle$ be the threshold without clustering and $T_0 + \delta T$ be the threshold found by including the correction due to triangles. From equation (10) it follows that

$$\frac{\delta T}{T_0} = \frac{2 \langle n_{\Delta} \rangle \langle k \rangle}{\langle k^2 - k \rangle^2} + \mathcal{O} \left(\left[\frac{2 \langle n_{\Delta} \rangle \langle k \rangle}{\langle k^2 - k \rangle^2} \right]^2 \right). \quad (11)$$

Because a given node of degree k is contained in at most $(k^2 - k)/2$ triangles, we conclude $2 \langle n_{\Delta} \rangle / \langle k^2 - k \rangle \leq 1$. So if $\langle k \rangle / \langle k^2 - k \rangle$ is small the leading order term of equation (11) is small and triangles do not significantly

²Early noise controls how quickly outbreaks become epidemics, and so once stochastic effects become small, the curves appear to be translations in time. We note that it is common to consider the temporal average of a number of outbreaks. However, prior to taking an average, the curves should be shifted in time so that they coincide once the stochastic effects are no longer important. Failure to do so underestimates the early growth, peak incidence, and late decay while it overestimates the epidemic duration. This can lead to an incorrect understanding of “typical” outbreaks.

alter the epidemic threshold regardless of the density of triangles. For the EpiSimS network, $\langle k \rangle / \langle k^2 - k \rangle$ takes the value 0.046, and so we do not anticipate clustering to play an important role in determining the threshold.

Above threshold, we assume that \mathcal{P} may be expanded much like (10)

$$\mathcal{P} = \mathcal{P}_0 + \mathcal{P}_1 \langle n_\Delta \rangle + \mathcal{P}_2 \langle n_\Delta \rangle^2 + \dots + Q_1 \langle n_\square \rangle + \dots \quad (12)$$

where \mathcal{P}_0 is the epidemic probability in a CM network of the same degree distribution. Although calculating $\mathcal{R}_{0,1}$ only requires information about nodes of distance at most two from the index case, \mathcal{P} may depend on effects occurring at larger distance, and so the expansion has many additional terms. In general, we expect that if the average degree is large, then the various coefficients of the correction terms are all small. The larger a structure is, the smaller we expect its corresponding coefficient to be. The coefficient for triangles \mathcal{P}_1 may be found by

$$\mathcal{P}_1 \langle n_\Delta \rangle = -\frac{1}{N} \sum_{u \in G} \sum_{\Delta \in G} \hat{p}_\Delta(u),$$

where $\hat{p}_\Delta(u)$ is the probability that a given triangle prevents an epidemic if u is the index case (regardless of whether u is part of the triangle). Reversing the order of summation we get

$$\mathcal{P}_1 \langle n_\Delta \rangle = -\frac{N_\Delta}{N} \left\langle \sum_{u \in G} \hat{p}_\Delta(u) \right\rangle_\Delta = -\frac{1}{3} \langle n_\Delta \rangle \left\langle \sum_{u \in G} \hat{p}_\Delta(u) \right\rangle_\Delta,$$

where N_Δ is the number of triangles in G and $\langle \cdot \rangle_\Delta$ is the average of the given quantity taken over all triangles. Thus

$$\mathcal{P}_1 = -\frac{1}{3} \left\langle \sum_{u \in G} \hat{p}_\Delta(u) \right\rangle_\Delta,$$

and we can find \mathcal{P}_1 by considering the average effect of a single triangle in an unclustered network.

To calculate the impact of a triangle with nodes u , v , and w on \mathcal{P} for a given network, we consider that triangle and a randomly chosen edge $\{x, y\}$ elsewhere in the network. If we replace the edges $\{v, w\}$ and $\{x, y\}$ with $\{v, x\}$ and $\{w, y\}$, then we have a new network without the triangle, but with the same degree distribution. We must estimate the expected change in \mathcal{P} caused by switching the edges.

We begin by assuming u is the index case. The triangle can affect \mathcal{P} only if the infection tries to cross all three edges, that is, if the infection process ‘loses’ an edge because of clustering. This may happen in three distinct ways. In the first, node u infects both v and w , and then v and/or w tries to infect the other. In the second u infects v but not w , then v infects w , and finally w tries to infect u . The third is symmetric to the second (with u infecting w).

To leading order we can ignore other short cycles, so the probability that an edge leading out of u (not to v or w) will not cause an epidemic is $g = 1 - T + Th$, where h (as before) is the probability that a randomly chosen secondary case does not cause an epidemic in an unclustered network and can be calculated using equation (9).

We perform a sample calculation with the first case: u infects both v and w . Assume that u has degree k_u , v has degree k_v , and w has degree k_w . The probability that u infects both v and w without some other edge leading from u , v , or w starting an epidemic is $T^2 g^{k_u+k_v+k_w-6}$. If the $\{v, w\}$ edge were broken and v and w were joined to x and y respectively (see figure 7), then the new probability of u to infect both v and w without an epidemic becomes $T^2 g^{k_u+k_v+k_w-4}$. The difference is $T^2 g^{k_u+k_v+k_w-6} (1-g^2)$, which is the product of three terms, all at most 1. If the sum $k_u + k_v + k_w$ is moderately large, then either $g^{k_u+k_v+k_w-6} \ll 1$ or $1-g^2 \ll 1$ (if g is not close to 1 then the first term is small, otherwise the second term is small). Thus the triangle has little impact on the epidemic probability in this case.³ Similar analysis applies to the other two cases where the w to u or v to u infections are lost. Provided the typical sum of degrees of nodes in

³If \mathcal{P} is small, then the *relative* change may be large, but the absolute change is small.



Figure 7: Replacing the edges $\{v, w\}$ and $\{x, y\}$ with $\{v, x\}$ and $\{w, y\}$ breaks the triangle and allows more infections, without affecting the degree distribution.

a triangle is relatively large, the probability of an epidemic when the index case is in the triangle is not impacted significantly.

If the index case is not part of the triangle, then the above analysis is modified because we must also consider each node in the path from the index case to the triangle. We must first calculate the probability that infection reaches a node in the triangle while simultaneously no intermediate node sparks an epidemic, and then we calculate the probability as above that the triangle prevents an epidemic. If the index case is u_1 and the path from u_1 to the triangle goes through u_2, \dots, u_n and then reaches u , then the probability that the triangle prevents an epidemic $\hat{p}(u_1)$ is given by $T^n(g^{-2n+\sum_i k_{u_i}})\hat{p}(u)$. This falls off very quickly, and so nodes not in the triangle are unimportant, unless typical degrees are small.

In contrast, in a network with small average degree and a significant number of triangles this becomes significant. This explains observations of [41, 40] who use networks with average degree less than 3 and find that clustering significantly alters \mathcal{A} .

It is tempting to generalise our conclusion and state that if the average degree is large, clustering has no impact on \mathcal{P} or \mathcal{A} . However, there are a number of counter-examples: consider a network made up of isolated cliques with N_c nodes, then in expansion (12) the coefficient for cliques of N_c nodes will not be small. Consequently care must be taken when using such an expansion to ensure that neglected terms resulting from larger scale structures are in fact negligible. For social networks, we generally anticipate this highly segregated situation to be unimportant.

We conclude that for most reasonable networks, clustering is only important for \mathcal{P} and \mathcal{A} if the typical degrees of nodes are low in which case \mathcal{R}_0 is small. A consequence of these results is that if \mathcal{R}_0 is moderately large, then \mathcal{P} and \mathcal{A} are effectively unaltered by clustering. If \mathcal{R}_0 is small, however, clustering may or may not play a role in determining \mathcal{P} and \mathcal{A} , depending on whether \mathcal{R}_0 is small because the degrees are small or because T is small.

4 Clustered networks with heterogeneous nodes

When we drop the assumption of constant transmissibility, disease spread becomes more complicated. If \mathcal{I} is heterogeneous and u infects a neighbour, then the *a posteriori* expectation for $T_{out}(u)$ becomes higher: it is likely to infect more neighbours. This accentuates the effect of short cycles, enhancing the impact of clustering on \mathcal{R}_0 , \mathcal{P} , and \mathcal{A} . A similar argument applies with heterogeneity in \mathcal{S} : if v is not infected by one of its neighbours, then the *a posteriori* expectation for $T_{in}(v)$ becomes lower: it is less likely to be infected by other neighbours, and so has multiple opportunities to prevent an epidemic. Again this accentuates the effect of short cycles.

In this section we investigate how varying the infectiousness and susceptibility of nodes in the EpiSimS network enables clustering to alter the values of \mathcal{P} and \mathcal{A} . We will make use of the *ordering assumption* and its consequences from [33]: if u_1 is “more infectious” than u_2 in a given instance [or v_1 “more susceptible”

Symbol	Infectiousness	Susceptibility
◆	$P(\mathcal{I}) = \delta(\mathcal{I} - 1)$	$P(\mathcal{S}) = 0.5\delta(\mathcal{S} - 0.001) + 0.5\delta(\mathcal{S} - 1)$
■	$P(\mathcal{I}) = 0.3\delta(\mathcal{I} - 0.001) + 0.7\delta(\mathcal{I} - 1)$	$P(\mathcal{S}) = \delta(\mathcal{S} - 1)$
×	$P(\mathcal{I}) = 0.5\delta(\mathcal{I} - 0.1) + 0.5\delta(\mathcal{I} - 1)$	$P(\mathcal{S}) = 0.2\delta(\mathcal{S} - 0.1) + 0.8\delta(\mathcal{S} - 1)$
●	$P(\mathcal{I}) = 0.5\delta(\mathcal{I} - 0.1) + 0.5\delta(\mathcal{I} - 1)$	$P(\mathcal{S}) = 0.8\delta(\mathcal{S} - 0.01) + 0.2\delta(\mathcal{S} - 1)$
◆	Maximally heterogeneous $P(T_{out}) = \langle T \rangle \delta(T_{out} - 1) + (1 - \langle T \rangle) \delta(T_{out})$	Homogeneous $T_{in} = \langle T \rangle$

Table 1: For the calculations of sections 4 and 5 we determine T_{uv} using equations (2) and (1) with the distributions of \mathcal{I} and \mathcal{S} given in the first four rows, or by considering a maximally heterogeneous population for which $\langle T \rangle$ of the population infects all neighbours and $1 - \langle T \rangle$ infect no neighbours. The function δ is the Dirac delta function.

than v_2], then u_1 is always more infectious than u_2 [or v_1 always more susceptible than v_2]. More specifically, the ordering assumption states that if $T_{out}(u_1) > T_{out}(u_2)$, then $T(\mathcal{I}_{u_1}, \mathcal{S}) \geq T(\mathcal{I}_{u_2}, \mathcal{S})$ for all \mathcal{S} , and the corresponding statement for T_{in} . The results of [33] show that if the ordering assumption holds, heterogeneity tends to reduce \mathcal{P} and \mathcal{A} , and the upper bounds on \mathcal{P} and \mathcal{A} correspond to homogeneous populations (constant T).

For simulations in this section, we consider five different illustrative cases, which will be denoted throughout by the symbol given in table 1. In the first four, we use equation (2) so that $T_{uv} = 1 - e^{-\alpha \mathcal{I}_u \mathcal{S}_v}$ with the distribution of \mathcal{I} and \mathcal{S} varying for each. We vary α to change the average transmissibility. In the fifth case the out-transmissibility is maximally heterogeneous: A fraction $\langle T \rangle$ of the population infect all neighbours, while the remaining $1 - \langle T \rangle$ infect no neighbours.

The fifth case gives a lower bound on \mathcal{P} for a homogeneously susceptible population [42]. It is hypothesised to remain a lower bound on \mathcal{P} if susceptibility is allowed to vary [33]. We could also consider maximal heterogeneity in susceptibility, but the results for \mathcal{P} and \mathcal{A} merely correspond to interchanging their values for maximal heterogeneity in infectiousness, and so we do not need to consider it explicitly.

4.1 The basic reproductive ratio

We use simulations to calculate the rank reproductive ratio $\mathcal{R}_{0,r}$ for the cases of table 1 and plot the result for $0 \leq r \leq 4$ in figure 8. Note that $\mathcal{R}_{0,1}$ remains a good approximation to \mathcal{R}_0 . In the first four cases, \mathcal{R}_0 is again asymptotic to the unclustered approximation as $\langle T \rangle \rightarrow 0$. There are small kinks for ◆ and ■ at $\langle T \rangle = 0.5$ and $\langle T \rangle = 0.7$ respectively, resulting from the nature of those distributions. The heterogeneities act to enhance the effect of clustering on \mathcal{R}_0 , but the effect is relatively small.

In the final, maximally heterogeneous case ◆, $\mathcal{R}_{0,1}$ remains a good approximation to \mathcal{R}_0 . At small values of $\langle T \rangle$, the heterogeneity causes clustering to have a larger impact than in a homogeneous population as seen in the lower right panel of figure 8, and so this is not asymptotic to the unclustered approximation. At larger values of $\langle T \rangle$ the heterogeneous and homogeneous growth rates are similar.

As before, we can calculate $\mathcal{R}_{0,1}$ analytically, which helps explain our observations. If the ordering assumption holds, we may use a simplified notation $T(T_{out}, T_{in})$ to denote the transmissibility from a node with out-transmissibility T_{out} to a node with in-transmissibility T_{in} .⁴ We have $\mathbb{E}[N_1] = \langle T \rangle \langle k \rangle$ and

$$\begin{aligned} \mathbb{E}[N_2] &= \frac{1}{N} \sum_u \sum_{v \neq u} \iint [1 - (1 - T_{out} T_{in})^{n_{uv}}] [1 - T(T_{out}, T_{in})]^{x_{uv}} Q_{out}(T_{out}) Q_{in}(T_{in}) dT_{out} dT_{in} \\ &= \langle k^2 - k \rangle \langle T \rangle^2 - 2 \langle n_{\Delta} \rangle \langle T_{out} T_{in} T(T_{out}, T_{in}) \rangle - \langle n_{\square} \rangle \langle T_{out}^2 \rangle \langle T_{in}^2 \rangle + \dots, \end{aligned}$$

and so we may express the growth rate as a perturbation about the unclustered case $\mathcal{R}_0 = \langle T \rangle \langle k^2 - k \rangle / \langle k \rangle$

⁴We can use this notation because the ordering assumption allows us to uniquely identify \mathcal{I} from T_{out} and \mathcal{S} from T_{in} . If the ordering assumption fails, similar results hold, but the notation is more cumbersome.

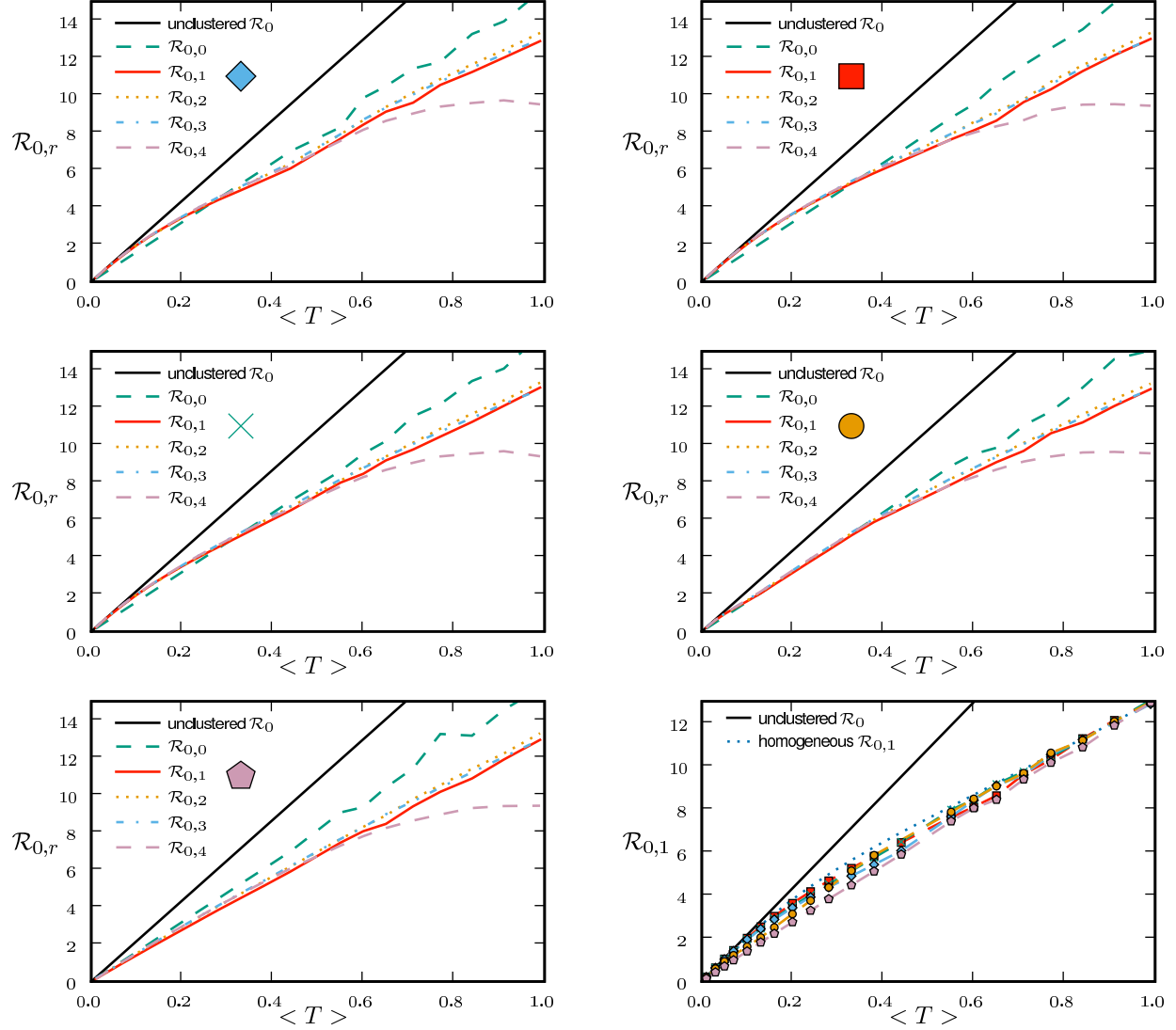


Figure 8: $\mathcal{R}_{0,r} = \mathbb{E}[N_{r+1}]/\mathbb{E}[N_r]$ calculated from simulations for the heterogeneous examples of table 1. The final panel (lower right) compares $\mathcal{R}_{0,1}$ for all of the different cases, including both unclustered and homogeneous.

giving

$$\mathcal{R}_{0,1} = \frac{\langle k^2 - k \rangle}{\langle k \rangle} \langle T \rangle - \frac{2 \langle n_{\Delta} \rangle \langle T_{out} T_{in} T(T_{out}, T_{in}) \rangle}{\langle k \rangle \langle T \rangle} - \frac{\langle n_{\square} \rangle \langle T_{out}^2 \rangle \langle T_{in}^2 \rangle}{\langle k \rangle \langle T \rangle} + \dots \quad (13)$$

For the second term, it may be shown that $\langle T \rangle^3 \leq \langle T_{out} T_{in} T(T_{out}, T_{in}) \rangle \leq \langle T \rangle^2$. The minimum occurs when T is constant, suggesting that the maximum growth rate occurs in a homogeneous population. The maximum $\langle T \rangle^2$ occurs either for \blacklozenge :

$$Q_{out}(T_{out}) = (1 - \langle T \rangle) \delta(T_{out}) + \langle T \rangle \delta(T_{out} - 1), \quad (14)$$

that is, when the out-transmissibility is maximally heterogeneous, or when the in-transmissibility is maxi-

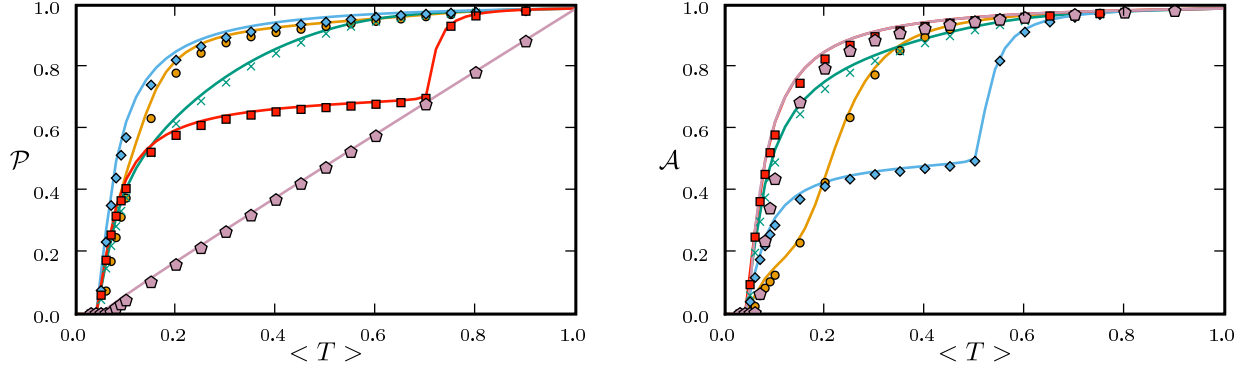


Figure 9: Comparison of \mathcal{P} and \mathcal{A} observed from simulations in the clustered EpiSimS network with heterogeneities (symbols) with that predicted by the unclustered theory (curves) using table 1. Each data point is based on a single EPN. For both \blacksquare and \blacklozenge $T_{in}(v) = \langle T \rangle$ for all nodes, and so the unclustered prediction for \mathcal{A} is the same.

maximally heterogeneous:

$$Q_{in}(T_{in}) = (1 - \langle T \rangle) \delta(T_{in}) + \langle T \rangle \delta(T_{in} - 1). \quad (15)$$

Consequently, we expect that for given $\langle T \rangle$ the minimum growth rate occurs with maximally heterogeneous infectiousness or susceptibility. These two minima for $\mathcal{R}_{0,1}$ have previously been hypothesised to give lower bounds on \mathcal{P} and \mathcal{A} respectively [33].

We note that in the maximally heterogeneous case, the correction term in (13) is significant at leading order in T . Consequently, if $\langle n_{\Delta} \rangle$ is comparable to $\langle k^2 - k \rangle / 2$ (that is, the clustering coefficient [43] is comparable to 1), the threshold value of $\langle T \rangle$ may be increased by clustering, and \mathcal{R}_0 is not asymptotic to the unclustered prediction as $\langle T \rangle \rightarrow 0$.

4.2 Probability and size

Figure 9 shows that the unclustered predictions provide a good estimate of \mathcal{P} and \mathcal{A} in the clustered EpiSimS network. We expect that in a network with sufficiently large average degree, the impact of clustering should once again be small.

We use arguments similar to before, taking a triangle with nodes u , v , and w . The reasoning becomes more difficult because knowledge that u infects v may increase the expectation that u infects w . Consequently the lost edges in triangles are more frequently encountered by the outbreak. However, the knowledge that u infects v also increases the expectation that u infects its other neighbours. For a triangle to prevent an epidemic, we need both that no edge outside the triangle leads to an epidemic and that the lost edge would otherwise have caused an epidemic. If the typical degree of the network is not small, then the fact that the lost edge is encountered more frequently may be offset by the fact that when it is encountered, other edges are more likely to spark an epidemic.

For \blacklozenge where nodes infect all or none of their neighbours, the effect of different triangles that share the index case cannot be separated as easily. The probability the index case directly infects a set of m nodes of interest is $\langle T \rangle$, rather than T^m . Thus expansions as in (12) do not work as well: terms that were previously higher order become significant. Close to the epidemic threshold, this can play an important role. However, well above the epidemic threshold, if the index case infects all of its neighbours, an epidemic is almost guaranteed and so $\mathcal{P} \approx \langle T \rangle$ regardless of whether the network is clustered. Thus for \blacklozenge , clustering affects \mathcal{P} only close to the epidemic threshold.

In the opposite case where nodes would be infected by any neighbour or else no neighbour, the values of \mathcal{P} and \mathcal{A} are interchanged. Thus for maximally heterogeneous susceptibility \mathcal{P} could be significantly altered close to the threshold. The reason for this is as follows: For the first step the spread is indistinguishable from

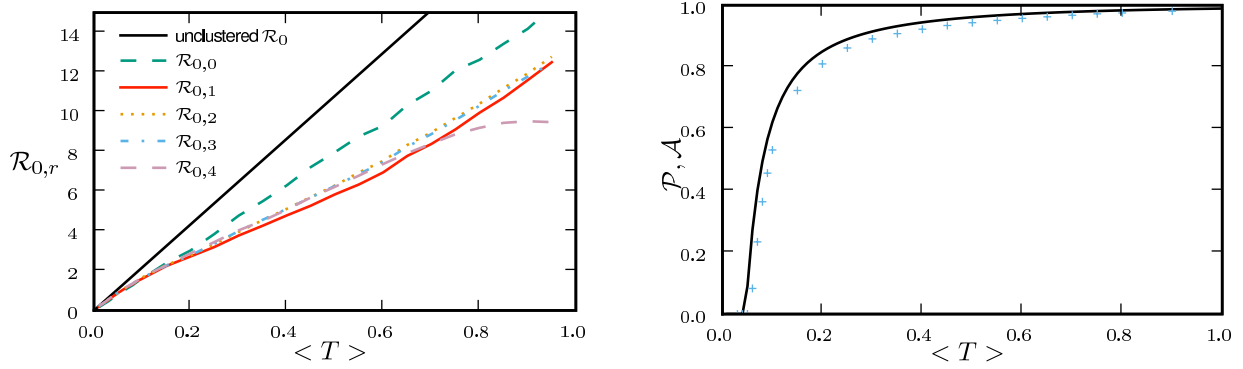


Figure 10: $\mathcal{R}_{0,r}$, \mathcal{P} , and \mathcal{A} for the weighted EpiSimS network with a homogeneous population.

that of an outbreak with constant T . However, when infections of rank 1 attempt to infect their neighbours, they cannot infect any of the neighbours of the index case. In contrast, in the constant T case, any neighbour not infected by the index case would be susceptible at later steps. Consequently, the impact of triangles becomes much more important (by a factor of $1/\langle T \rangle$) and our earlier argument for neglecting them fails. The interaction of maximal heterogeneity with clustering in this case is larger, but it nevertheless becomes unimportant far from the threshold.

Our prediction that heterogeneity allows clustering to be more significant close to the threshold is borne out for \bullet where there is relatively strong heterogeneity in susceptibility just above the epidemic threshold. The epidemic threshold for \bullet is increased compared to the other cases. In contrast there is much stronger heterogeneity in susceptibility for \blacklozenge at $\langle T \rangle = 0.5$ and in infectiousness for \blacksquare at $\langle T \rangle = 0.7$. This results in a reduction in \mathcal{A} and \mathcal{P} respectively, but because it is far from threshold, there is little deviation from the unclustered predictions.

5 Clustered networks with weighted edges

When we allow edges to be weighted, new complications arise. The weights we use in our simulations are the durations of contacts from the EpiSimS simulation and are discussed in detail in D. If a contact in the original EpiSimS simulation is longer, a higher weight is assigned. If the weights of different edges were independent, then we could simply take $T_{uv} = \int T(\mathcal{I}_u, \mathcal{S}_v, w)P(w)dw$. However, edge weights are not independent: clustered connections tend to have larger weights. If brief contacts are negligible, the disease spreads on a subnetwork of the original network. The new network has a comparable number of short cycles to the original, but lower typical degree. This should enhance the impact of clustering.

For our calculations in this section, we first isolate the impact of weighted edges by taking a homogeneous population ($\mathcal{I} = \mathcal{S} = 1$) and using $T_{uv} = 1 - e^{-\alpha w_{uv}}$. We vary α in order to set $\langle T \rangle$. We then investigate a heterogeneous population using equation (1) with the first four distributions of table 1.

Results for a homogeneous population are shown in figure 10. Because $T_{uv} = T_{vu}$ for all pairs, it follows that $\mathcal{P} = \mathcal{A}$. If different edge weights were uncorrelated, then the value of \mathcal{R}_0 would match with figure 2 and \mathcal{P} and \mathcal{A} would match with figure 6. We see, however, that \mathcal{R}_0 is significantly reduced from the homogeneous unweighted population (but $\mathcal{R}_{0,1}$ remains a good approximation). Close to the threshold \mathcal{P} and \mathcal{A} are mildly reduced. These observations are consistent with our expectation that clustering should be accentuated by incorporating edge weights. Although the predictions for \mathcal{P} and \mathcal{A} are not far off, we expect that they would improve if we adjusted the degree distribution to match that of the effective network on which the disease spreads.

When the population is moderately heterogeneous (figure 11), we still find that $\mathcal{R}_{0,1}$ is a reasonable approximation to the true value of \mathcal{R}_0 , however, it slightly underestimates \mathcal{R}_0 as $\langle T \rangle$ grows. Unfortunately

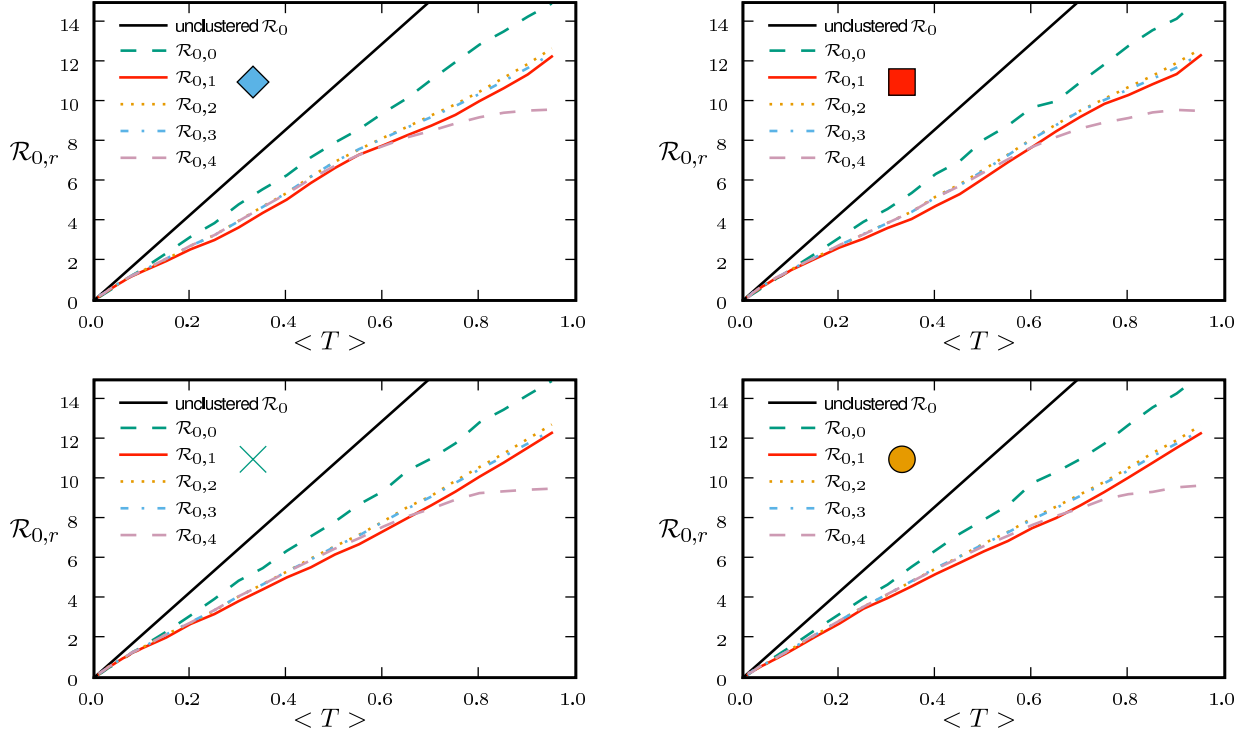


Figure 11: $\mathcal{R}_{0,r}$ with heterogeneous transmissibility and weighted edges on the EpiSimS network.

the analytic calculation of $\mathcal{R}_{0,1}$ is much more difficult, and so it is more appropriate to use simulations to estimate its value. If there were no correlation between weights of different edges, then the calculation would reduce to that of section 4.

We consider \mathcal{P} and \mathcal{A} in figure 12. The unclustered predictions are reasonable approximations of the actual values. The error is larger than before because we have combined two effects (edge weights and heterogeneity) that both accentuate the impact of clustering. In spite of this, the predicted values of \mathcal{P} and \mathcal{A} are not far off, and the direction of the error is consistent: the unclustered prediction is always an overestimate.

6 Discussion

We have investigated the interplay of clustering, node heterogeneity, and edge weights on the growth rate \mathcal{R}_0 , probability \mathcal{P} , and size of epidemics \mathcal{A} in social networks. For unclustered networks with independently distributed edge weights, it is possible to predict all these quantities analytically. Under weak assumptions we can accurately estimate \mathcal{R}_0 , \mathcal{P} , and \mathcal{A} for clustered networks.

If the typical degrees are not small, then for a given average transmissibility and degree distribution:

- The dominant effect controlling the growth rate of epidemics is clustering. Increased clustering reduces \mathcal{R}_0 .
- The dominant effect controlling the probability of epidemics is heterogeneity in infectiousness. Increased heterogeneity reduces \mathcal{P} .

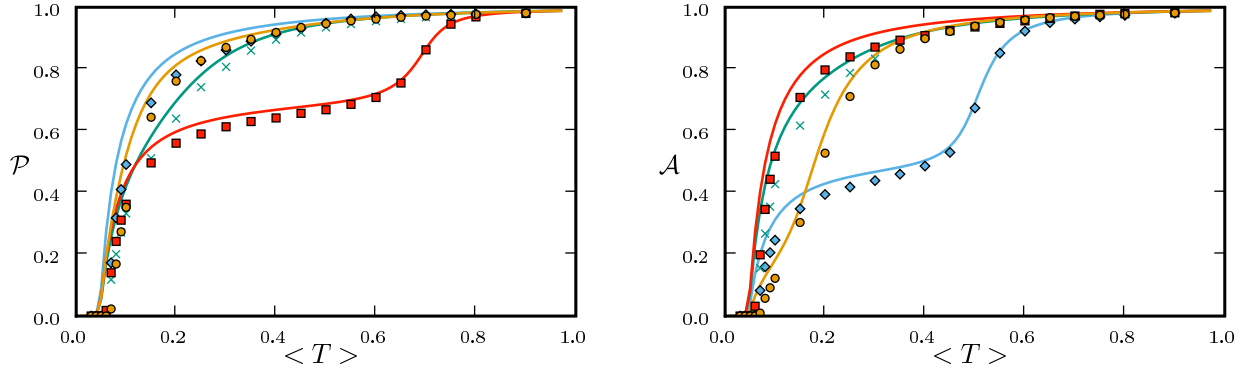


Figure 12: Simulated \mathcal{P} and \mathcal{A} (symbols) for the weighted EpiSims network compared with predictions in unclustered networks with the same edge weight distribution (curves).

- The dominant effect controlling the size of epidemics is heterogeneity in susceptibility. Increased heterogeneity reduces \mathcal{A}

We are thus able to neglect clustering and still closely estimate \mathcal{P} based only on the degree distribution and the out-transmissibility pdf Q_{out} . The estimate for \mathcal{A} depends only on degree distribution and the in-transmissibility pdf Q_{in} . The impact of clustering is significant in altering \mathcal{R}_0 , and its impact is mildly enhanced by heterogeneities. This enhancement occurs because the probability of following all edges of a cycle is increased if some of the edges are correlated due to the heterogeneity. If heterogeneity is large, clustering may play a small role in moving the epidemic threshold, but otherwise its effect on the threshold is negligible. In networks with small typical degree, it has been observed that clustering can modify \mathcal{P} or \mathcal{A} [41, 40], which is consistent with our estimates.

If edge weights are included, but are independently distributed, then their impact is in modifying $Q_{in}(T_{in})$ and $Q_{out}(T_{out})$. The resulting modification may be calculated explicitly, and edge weights have no further effect. If edge weights are correlated, they have a more important role in governing the behaviour of epidemics, particularly if higher weight edges tend to be the clustered edges (as frequently occurs in social networks). If this happens, then the impact of clustering is enhanced, and the growth rate of epidemics is further reduced.

When we move from predicting \mathcal{P} and \mathcal{A} to predicting \mathcal{R}_0 , we find that the growth rate is well approximated by $\mathcal{R}_{0,1} = \mathbb{E}[N_2]/\mathbb{E}[N_1]$. This may be calculated analytically in the homogeneous case (constant T). When heterogeneities are included, the calculation becomes harder, and when edge weights are included it becomes largely intractable. However, these are easily estimated through simulation.

These observations show that using \mathcal{R}_0 to predict \mathcal{A} will generally be inadequate. In a homogeneous but clustered population, \mathcal{R}_0 is reduced but \mathcal{A} is unaffected, and so predictions of \mathcal{A} based on \mathcal{R}_0 will be too small. In networks that are not clustered but have heterogeneities in susceptibility, \mathcal{R}_0 is unaffected but \mathcal{A} is substantially reduced. Consequently, the value of \mathcal{A} predicted from \mathcal{R}_0 will be too large.

Perhaps our most important conclusion about clustering is that it plays an important role in altering the growth of an epidemic, but it only plays a small role in determining whether an epidemic may occur or how big it would be. If the relevant questions are, “how likely is an epidemic and how large would it be?” then the modeller may proceed ignoring clustering. If however, the question is “how fast will an epidemic grow?” then clustering must be considered, but only enough to calculate $\mathcal{R}_{0,1}$.

Our results have implications for designing intervention strategies. A number of strategies are available to control epidemic spread, including travel restrictions, quarantines, and vaccination. Most of the mathematical theory predicting the effects of these strategies has been developed under the assumption of no clustering. Most immediately, if we measure $\mathcal{R}_0 = 2$ at the early stages of an epidemic, traditional approaches will suggest that vaccinating just over half of the population will bring the epidemic below threshold. However, if the population is clustered, then the observed \mathcal{R}_0 was already affected by the fact that some transmission

chains were redundant. Following vaccination, some of these chains will no longer be redundant and the disease may still spread with $\mathcal{R}_0 > 1$.

Achieving a better understanding of the effect of clustering further helps to guide our intuition when choosing between strategies. For example, let us assume that we have the choice between two strategies: in the first, we stagger work schedules in such a way that a typical person’s contacts is reduced by 1/3; in the second, we implement population-wide behavior changes so that the same reduction in number of contacts is achieved, but the work contacts are unaltered. The first reduces clustering while the second increases the relative frequency of clustering. The value of \mathcal{R}_0 is much smaller in the second case than in the first because of the larger clustering, but \mathcal{P} and \mathcal{A} are reduced by a comparable amount in both cases. Which strategy is best depends on our goals and relative costs.

Strategies that enhance heterogeneity in infectiousness or susceptibility can be important to help reduce \mathcal{P} or \mathcal{A} , even when there is little impact on \mathcal{R}_0 . Depending on which quantity we want to minimize, different choices will be optimal. Consider a choice between vaccinating all individuals with a vaccine that reduces T_{uv} by a factor of 1/2 for all pairs u and v or a contact tracing strategy that will remove 1/2 of all new infections before they have a chance to infect anyone. Both strategies reduce $\langle T \rangle$ by a half. However, the first reduces T_{out} uniformly, while the second increases heterogeneity in T_{out} . Thus if we have the choice of the two strategies, contact tracing is more likely to eliminate the disease before an epidemic can happen. If our choice is instead between a global vaccine reducing T_{in} by a factor of 1/2 for all individuals, or a completely effective vaccine that is only available for 1/2 of the population, the latter choice will be more effective for reducing \mathcal{A} .

Acknowledgements

This work was supported by the Division of Mathematical Modeling at the UBC CDC under CIHR (grants no. MOP-81273 and PPR-79231) and the BC Ministry of Health (Pandemic Preparedness Modeling Project), by DOE at LANL under Contract DE-AC52-06NA25396 and the DOE Office of ASCR program in Applied Mathematical Sciences, and by the RAPIDD program of the Science & Technology Directorate, Department of Homeland Security and the Fogarty International Center, National Institutes of Health. Luís M. A. Bettencourt contributed greatly to the early development of this work. I am grateful to Sara Y del Valle for providing the EpiSimS network data.

A Epidemic Percolation Networks

In this appendix, we describe the *Epidemic Percolation Network* (EPN), a tool that allows us to consider an epidemic as a static object rather than a dynamically changing process. This eases the understanding of certain key features and provides an improved technique to efficiently estimate \mathcal{P} . EPNs have received moderate use recently [23, 22, 33], and a precursor appeared in [26]. A sample EPN for an Erdős–Rényi network of average degree 3 and $T = 0.4$ is shown in figure 13.

Typically to estimate \mathcal{P} in an SIR model many Monte Carlo simulations are performed. This process requires many iterations to have confidence in the results. Representative results from 500 such simulations are found in figure 14. Note that there is considerably more noise in the estimates of \mathcal{P} than in the estimates of \mathcal{A} .

Instead we generate a single EPN \mathcal{E} . We first assign \mathcal{I} and \mathcal{S} to each node and (if necessary) w to each edge.⁵ Then for each node u and neighbour v we calculate T_{uv} and place the directed edge (u, v) into \mathcal{E} with probability T_{uv} . The distribution of out-components of a given node is the same as for the final outbreak following an introduced infection of that node in the original epidemic model.

⁵It is important that this assignment occur prior to infection [or at least independent of outbreak history]. If the infectiousness of v depends on the infectiousness of the node that infected v , then these results fail. This is the *time-homogeneity* assumption of [22] and is also used by [26]. Some effects that can occur when this assumption is false appear in [18].

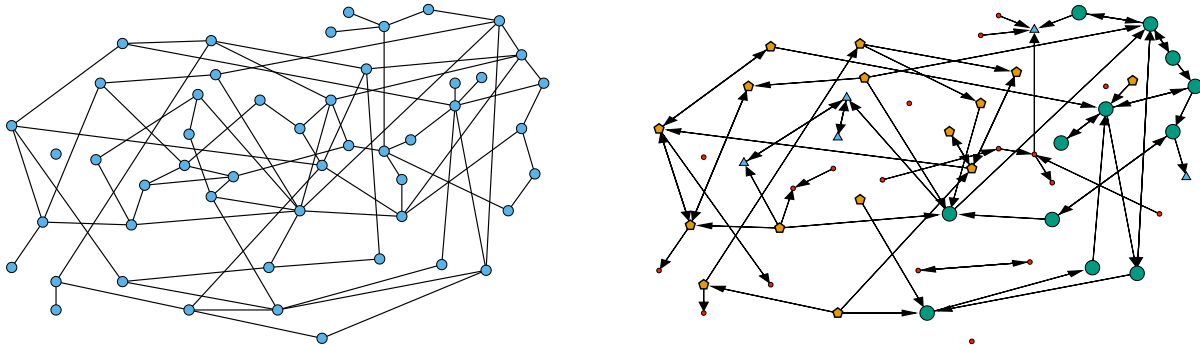


Figure 13: The underlying network for figure 1 and an EPN that leads to the same outbreak. Nodes in the G_{scc} are denoted by large circles, nodes in the G_{in} (but not in the G_{scc}) are denoted by pentagons, nodes in the G_{out} (but not in the G_{scc}) are denoted by triangles, and nodes not in any of these components are denoted by small circles.

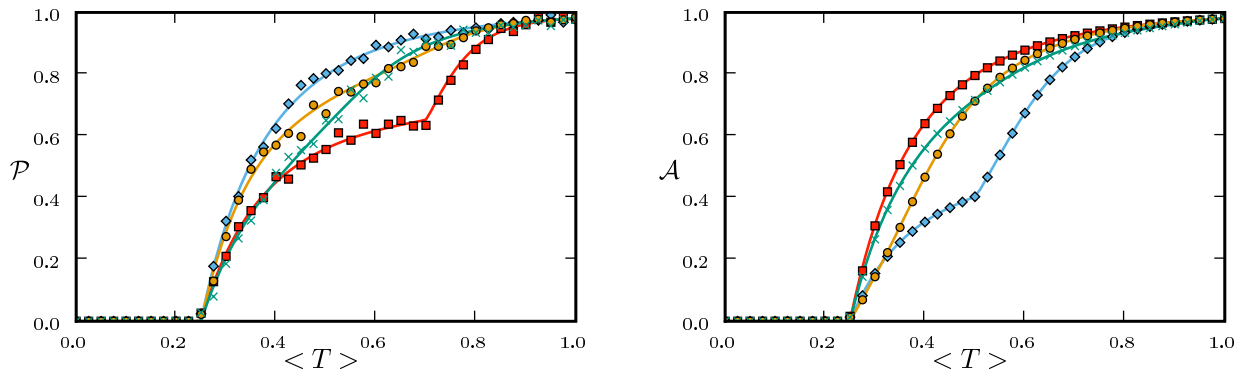


Figure 14: \mathcal{P} and \mathcal{A} in an Erdős-Rényi network of 10^5 nodes and $\langle k \rangle = 4$. Theory (curves) compare well with results of 500 simulations (symbols). We take $T_{uv} = 1 - e^{-\alpha \mathcal{I}_u \mathcal{S}_v}$, with distributions of \mathcal{I} and \mathcal{S} as given in table 1.

If the system is above the epidemic threshold, then \mathcal{E} will (almost surely) have a giant strongly connected component G_{scc} [9, 13]. We follow [13] and define the set of nodes (including G_{scc}) from which G_{scc} may be reached following the directed edges to be the giant in-component G_{in} . We symmetrically define G_{out} to be the set of nodes reachable from G_{scc} . Note that $G_{scc} = G_{in} \cap G_{out}$. If the initial infection is in G_{in} , an epidemic occurs, and all nodes in G_{out} become infected. Thus the size of G_{in} corresponds to the probability of an epidemic \mathcal{P} and the size of G_{out} corresponds to the size of an epidemic \mathcal{A} . This may be seen by comparing the EPN in figure 13 with the outbreak shown in figure 1.⁶

Thus in the limit of large networks, epidemic probability is well-approximated by $\mathcal{P} = |G_{in}|/|G|$ while the fraction infected is well-approximated by $\mathcal{A} = |G_{out}|/|G|$. This observation allows us to estimate \mathcal{P} from a single EPN (figure 15), rather than from hundreds of simulations (figure 14). If the structure of the network is sufficiently random, the error in \mathcal{P} and \mathcal{A} from a single EPN is $\mathcal{O}(\log N/N)$ (see, *e.g.*, [7]), and so in a large population a single simulation will provide a sufficiently good estimate.

⁶It is possible that a small number of nodes outside of G_{out} are infected, but the proportion vanishes as $|G| \rightarrow \infty$.

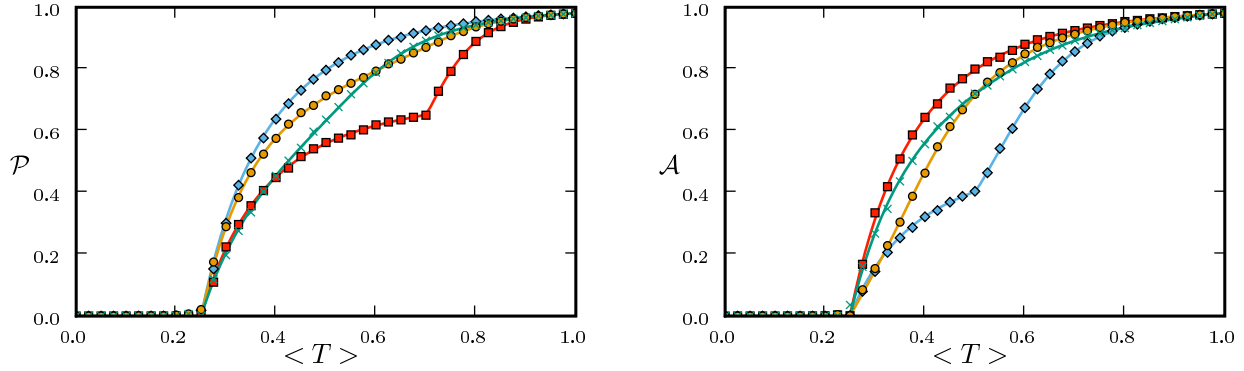


Figure 15: Same as figure 14, but calculated through a single EPN for each T . The noise is substantially reduced in the \mathcal{P} calculations, but slightly increased in the \mathcal{A} calculations.

B The basic reproductive ratio

In this appendix we provide examples demonstrating the need for the more careful definition of \mathcal{R}_0 in section 2, and we explore properties of this definition.

A pair of simple examples demonstrates the difficulties with the standard definition. In our first example, the standard definition suggests no epidemic is possible ($\mathcal{R}_0 < 1$), while in fact they are. In our second example, the standard definition suggests epidemics are possible ($\mathcal{R}_0 > 1$), while in fact they are not.

For the first example, consider a fully-connected population of $|G| \gg 1$ nodes. We add $3|G|$ isolated nodes and consider a disease for which $T = 3/|G|$. A node in the connected component will infect on average 3 nodes, while an isolated node infects none. On average therefore, a random index case infects 0.75 other nodes. Under the standard definition $\mathcal{R}_0 = 0.75$ and epidemics should be impossible. However, if the index case is in the connected component, the introduction is likely to lead to an epidemic.

Alternately, consider a population of $|G|$ nodes with each node having three neighbours. For simplicity we assume no short cycles. Assume that a disease spreads with probability $p \in (1/3, 1/2)$ to a given neighbour. The average number of secondary infections caused by a single introduced infection is $3p > 1$, giving $\mathcal{R}_0 > 1$ under the standard definition. However, each secondary infection has only two susceptible neighbours, and so infects on average $2p < 1$ neighbours, and the outbreak dies out.

Some of these issues have been dealt with by [12], who considered compartmental deterministic models of several types of individuals. At early time nonlinear terms are unimportant, and the profile of the infected population aligns with the eigenvector of the “next-generation” matrix. In stochastic settings, the same alignment occurs, but it may do so more quickly or slowly than predicted and for some realisations it may instead die out. To make a more rigorous definition of \mathcal{R}_0 , we turn to statements about the average behaviour. We set

$$\mathcal{R}_{0,r} = \frac{\mathbb{E}[N_{r+1}]}{\mathbb{E}[N_r]}$$

to be the ratio of the expected number of infections in rank $r + 1$ to the expected number in rank r . This value is affected by local small-scale structures. If the network is small, it is also affected by the finite size of the network, but if the network is large enough relative to r , we expect that the value will be unaffected by large-scale structure. In more concrete terms, the early growth of a disease in a neighbourhood is unaffected by whether that neighbourhood is part of a city of 100000, 1 million, or 10 million. As the disease spreads further, the effect of the finite city size will be noticeable for the smaller cities first. If the population is large enough, the ratio converges before the finite size has any impact. We define \mathcal{R}_0 mathematically as

$$\mathcal{R}_0 = \lim_{r \rightarrow \infty} \lim_{|G| \rightarrow \infty} \mathcal{R}_{0,r}. \quad (16)$$

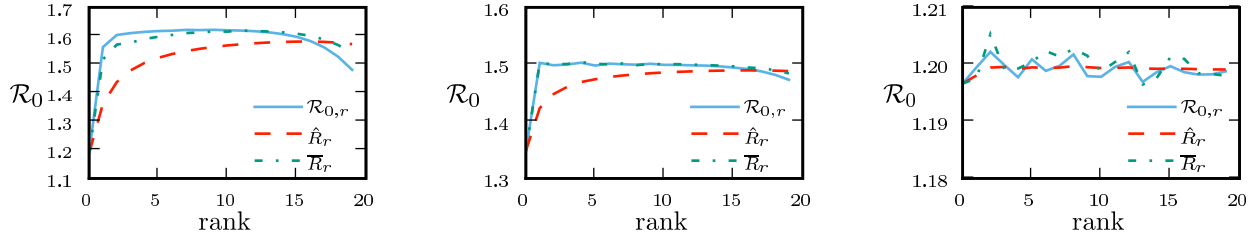


Figure 16: A comparison of the convergence of $\mathcal{R}_{0,r}$, \hat{R}_r , and \bar{R}_r for epidemics in the EpiSimS network ($T = 0.075$), an unclustered bimodal network ($T = 0.3$ with each node’s degree coming either from a Poisson distribution peaked at 3 or a Poisson distribution peaked at 6), and an Erdős–Rényi network ($T = 0.3$, average degree 4). The calculations used 10^5 simulations for each network. Note the difference in vertical scales.

This definition is similar to that of [42], who used

$$\begin{aligned} \hat{R}_r &= \mathbb{E}[N_{r+1}]^{1/(r+1)} \\ \mathcal{R}_0 &= \limsup_{r \rightarrow \infty} \limsup_{|G| \rightarrow \infty} \hat{R}_r, \end{aligned} \quad (17)$$

which is the limit as $r \rightarrow \infty$ of the geometric mean of $\mathcal{R}_{0,1}, \dots, \mathcal{R}_{0,r-1}$ (assuming the limit exists). This definition is more general and will converge in some cases where (16) does not. However, if (16) does converge (and typically we see that it does), then it reaches the same value, but does so sooner. So to clearly see \mathcal{R}_0 from (17), we must have a larger network.

Another suitable definition would be

$$\begin{aligned} \bar{R}_r &= \mathbb{E}[N_{r+1}/N_r] \\ \mathcal{R}_0 &= \lim_{r \rightarrow \infty} \lim_{|G| \rightarrow \infty} \bar{R}_r, \end{aligned} \quad (18)$$

where the expectation is taken over realisations with $N_r \neq 0$. This will tend to require more steps to converge because it counts small outbreaks equally with large outbreaks, and so outbreaks which have not yet grown and are dominated by stochastic effects would be as important to the average as well-established epidemics.

A comparison of these three definitions of \mathcal{R}_0 is shown in figure 16. They all result in similar values for \mathcal{R}_0 . For a clustered network, equation (16) converges more quickly. For large unclustered networks, $\mathcal{R}_{0,r} = \bar{R}_r$ and both converge to \mathcal{R}_0 at $r = 1$ while \hat{R}_r takes longer. In an Erdős–Rényi network, all three definitions give $\mathcal{R}_{0,r} = \mathcal{R}_0$ for all r ; only noise due to insufficient simulations affects the calculation.

To be fully rigorous, the $|G| \rightarrow \infty$ limit must be appropriately defined. It does not make sense to talk about $|G| \rightarrow \infty$ for a given network, and we cannot simply add nodes to the pre-existing network. We must take a sequence of networks in such a way that the small-scale structure is preserved, and as the network size grows, the size of the preserved structure increases.

To make this rigorous, we follow [33]. Take a sequence of finite networks G_n , with $|G_n| \rightarrow \infty$ as $n \rightarrow \infty$. We define B_r to be the network induced on the set of nodes within distance r of a central node. The sequence of networks is taken so that the probability that the structure surrounding a randomly chosen central node is isomorphic to a given B_r is the same for all G_n if $n \geq r$. This means that the small-scale structure in the different networks is the same, and the size of what is considered “small-scale” increases with n .

We note that although the $|G| \rightarrow \infty$ limit may be well-defined, it is possible that the $r \rightarrow \infty$ limit in (16) does not converge. This may occur because, for example, growth within a neighbourhood may happen at one rate, while spread between neighbourhoods in a suburb may happen at another, and spread between suburbs in a city may happen at yet another. If the rate of spread continues to change as the grouping size changes, then the $r \rightarrow \infty$ limit may not exist. An effect analogous to this may appear in [1] which considered

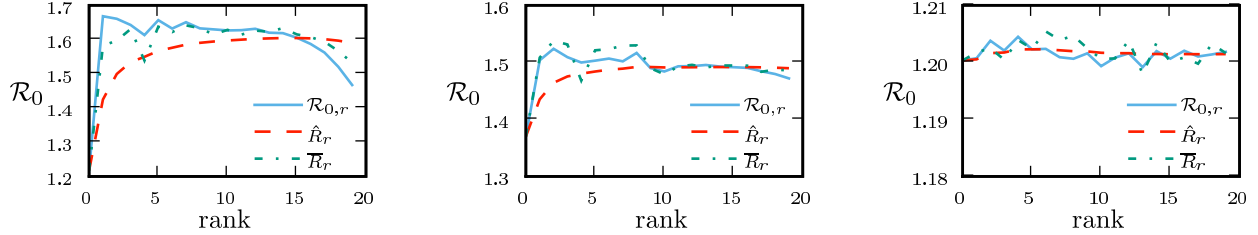


Figure 17: A comparison of the convergence of $\mathcal{R}_{0,r}$, \hat{R}_r , and \bar{R}_r for the same networks and conditions as in figure 16 except using a single EPN for each data point with 10^5 different index cases within that EPN rather than 10^5 distinct simulations [actually at submission the first two plots used only 10^3 index cases, more will be added when calculations complete].

disease spread in Italy. Two distinct growth rates are seen depending on whether the disease is spreading in the general country or in Rome.

Finally, it is possible to estimate \mathcal{R}_0 using a single EPN rather than multiple simulations. This is a much faster process, and so it is possible to do many more simulations to reduce the noise. However, because it is chosen from a single EPN, there may be a small systematic error. In figure 17, we plot the values for the same conditions as in figure 16. We use the same number of index cases and so the noise is comparable. The value of \mathcal{R}_0 is not noticeably affected by choosing a single EPN rather than multiple simulations. In the calculations in the paper, we have used a single EPN rather than multiple simulations.

C Epidemics in Configuration Model Networks

We briefly review previous work for epidemic spread in CM networks. These are the simplest networks to investigate, and so the theory has been developed further than for other networks [3, 36, 30, 23, 32, 39, 28]. See [33, 40] for some discussion of more arbitrary unclustered networks.⁷ We extend the earlier theory by allowing independently assigned edge weights.⁸

C.0.1 The basic reproductive ratio

Early in the spread of an infectious disease on a CM network, the probability of a node becoming infected is proportional to its degree, and so the pdf for the degree of infected nodes is $kP(k)/\langle k \rangle$. We choose an infected node u with degree k uniformly from nodes of rank r . If the network is large enough that we can ignore short cycles, then all of u 's neighbours are susceptible except the node which infected u . Thus u may infect up to $k-1$ neighbours. The probability $T_{out}(u)$ that u will infect a randomly chosen neighbour is chosen from $Q_{out}(T_{out})$, and so the probability u infects exactly $j \leq k-1$ neighbours is $\binom{k-1}{j} T_{out}^j (1-T_{out})^{k-1-j}$. Integrating this over possible values of T_{out} and summing over k and j , we find that for $r > 0$ the rank reproductive ratio is

$$\mathcal{R}_{0,r} = \frac{1}{\langle k \rangle} \sum_{k=1}^{\infty} \left(kP(k) \sum_{j=0}^{k-1} j \int \binom{k-1}{j} T_{out}^j (1-T_{out})^{k-1-j} P(T_{out}) dT_{out} \right) = \langle T \rangle \frac{\langle k^2 - k \rangle}{\langle k \rangle},$$

and so

$$\mathcal{R}_0 = \langle T \rangle \frac{\langle k^2 - k \rangle}{\langle k \rangle} \quad (19)$$

⁷Perhaps the most significant result for non-CM networks is that if the higher degree nodes preferentially contact other high degree nodes, then the threshold transmissibility for an epidemic is reduced.

⁸If edge weights are not assigned independently, then infection along different edges is not independent, and the methods of this section do not apply.

Thus we find that for CM networks⁹ $\mathcal{R}_0 \neq \mathcal{R}_{0,0} = \langle T \rangle \langle k \rangle$.

C.0.2 Probability and size

We look for the probability that a single infected node causes a chain of infections leading to an epidemic. Because interchanging edge direction in an EPN interchanges \mathcal{P} and \mathcal{A} , we may focus on calculating \mathcal{P} . Equivalent techniques replacing T_{out} by T_{in} below give \mathcal{A} . Our analysis is performed in the infinite network limit.

We set f to be the probability a randomly chosen index case does not start an epidemic. We find

$$f = \sum_k \left(P(k) \int_{T_{out}} [1 - T_{out} + T_{out}h]^k P(T_{out}) dT_{out} \right),$$

where h is the probability a randomly chosen secondary case does not start an epidemic. The value of h satisfies the recurrence relation

$$h = \frac{1}{\langle k \rangle} \sum_k \left(kP(k) \int_{T_{out}} [1 - T_{out} + T_{out}h]^{k-1} P(T_{out}) dT_{out} \right).$$

If $\mathcal{R}_0 < 1$, the trivial solution $f = h = 1$ is the only solution. For $\mathcal{R}_0 > 1$ an additional solution appears and is the physically relevant root. From this we can calculate $\mathcal{P} = 1 - f$.

Note that \mathcal{P} depends on the distribution of T_{out} , but is not affected by the distribution of T_{in} . Similarly, \mathcal{A} depends on the distribution of T_{in} but is not affected by the distribution of T_{out} . This result holds for unclustered, but not for clustered, networks.

C.0.3 Summary

We have shown that for CM networks, $\mathcal{R}_0 = \langle T \rangle \langle k^2 - k \rangle / \langle k \rangle$. In particular it depends only on the network properties and the average transmissibility. In contrast, the probability \mathcal{P} and size \mathcal{A} are affected by the details of the distribution. Intuitively, this is easy to understand. For example, if we consider \mathcal{A} in populations with varying T_{in} , at early times the rate of growth is governed by the average number of new infections created, which depends on the average transmissibility. However, a disproportionate number of highly susceptible nodes are infected, and so the average T_{in} of remaining nodes drops. By the end of the epidemic nodes are much harder to infect than they would have been if all were equally susceptible initially, and so the epidemic infects fewer people.

A consequence of this is that we cannot predict \mathcal{A} based only on the early growth rate. Although this is frequently done (see for example [27] and references therein), these calculations usually assume that the population is homogeneously susceptible, which is not always the case, particularly when a vaccine or previous exposure to similar diseases exists.

D The EpiSimS Network

We consider a network produced by EpiSimS for Portland, Oregon [11, 15, 5]. This simulation uses Census data, road structure, building locations, and population surveys to construct a virtual population that travels through the city. From the activity of individuals in the simulation, we may reconstruct who was in contact with whom and for how long.

There are 1615860 nodes in the network, of which 1591010 are in the giant component. The average degree is approximately 16, and the average squared degree is approximately 359. The degree distribution has an exponential tail, and clustering is concentrated in the low-degree nodes. For our approximations of \mathcal{R}_0 , we also need information about length 2 paths. We calculate the number of pairs of nodes with each

⁹Unless the degree distribution satisfies $\langle k^2 - k \rangle = \langle k \rangle^2$. The best-known such networks are Erdős-Rényi networks which have a Poisson degree distribution in the limit of large network size.

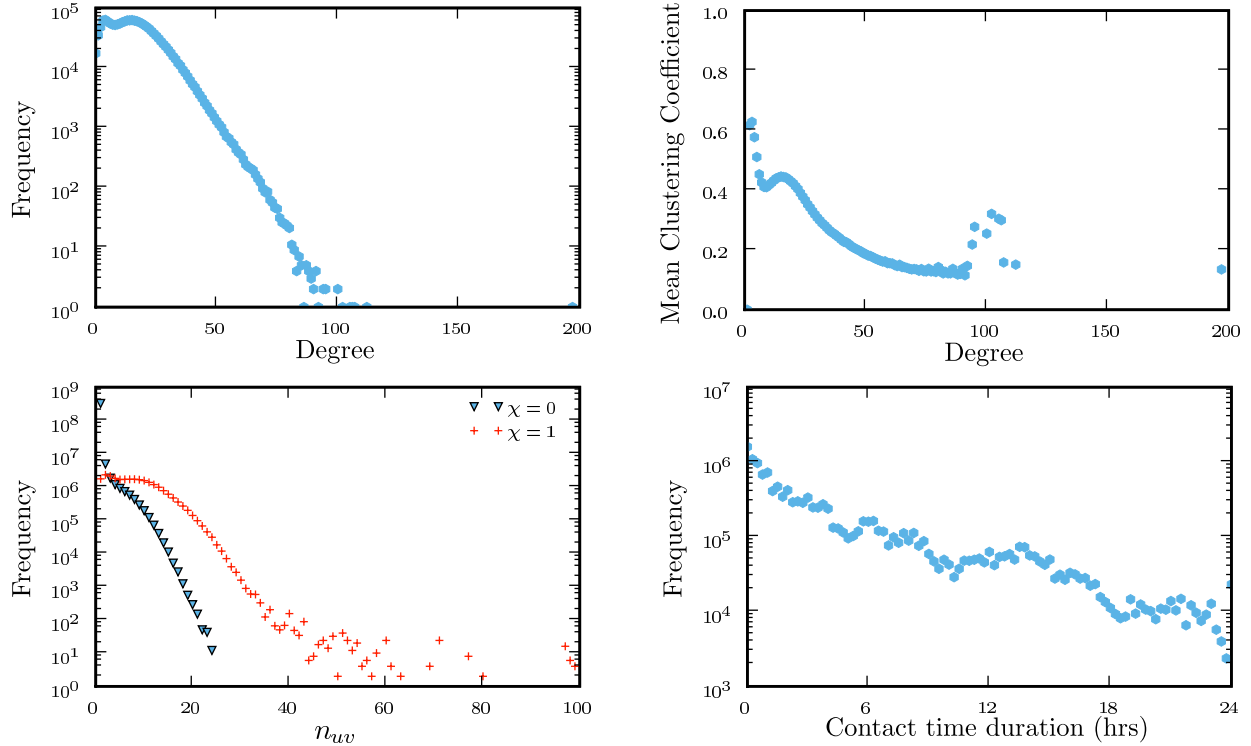


Figure 18: Properties of the EpiSimS network. For the final plot, contact times are binned in quarter hour increments, but exact values were used in calculations.

value of n_{uv} for which $\chi_{uv} = 0$ and $\chi_{uv} = 1$. Large values of n_{uv} are more frequent when $\chi_{uv} = 1$. The distribution of edge weights is fairly broad. Many contacts are very short, but the number of long contacts is not negligible.

References

- [1] M. Ajelli and S. Merler. The impact of the unstructured contacts component in influenza pandemic modeling. *PLoS ONE*, 3(1):e1519, 2008.
- [2] Roy M. Anderson and Robert M. May. *Infectious Diseases of Humans*. Oxford University Press, Oxford, 1991.
- [3] Håkan Andersson. Limit theorems for a random graph epidemic model. *Annals of Applied Probability*, 8:1331–1349, 1998.
- [4] Shweta Bansal. *Ecology of Infectious Diseases with Contact Networks and Percolation Theory*. PhD thesis, University of Texas at Austin, 2008.
- [5] C. L. Barrett, S. G. Eubank, and J. P. Smith. If smallpox strikes Portland. . . . *Scientific American*, 292(3):42–49, 2005.
- [6] B. Bollobás. A probabilistic proof of an asymptotic formula for the number of labelled random graphs. *European Journal of Combinatorics*, 1:311–316, 1980.

- [7] B. Bollobás. *Random Graphs*. Cambridge University Press, 2001.
- [8] Tom Britton, Maria Deijfen, Andreas Nordvall Lagerås, and Mathias Lindholm. Epidemics on random graphs with tunable clustering. *Arxiv preprint arXiv:0708.3939*, 2007.
- [9] Andrei Broder, Ravi Kumar, Farzin Maghoul, Prabhakar Raghavan, Sridhar Rajagopalan, Raymie Stata, Andrew Tomkins, and Janet Wiener. Graph structure in the web. *Computer Networks*, 33:309–320, 2000.
- [10] Sara Y Del Valle, J. Mac Hyman, Herbert W. Hethcote, and Stephen G. Eubank. Mixing patterns between age groups in social networks. *Social Networks*, 29(4):539–554, 2007.
- [11] Sara Y Del Valle, Phillip D. Stroud, James P. Smith, Susan M. Mniszewski, Jane M. Riese, Stephen J. Sydoriak, and Deborah A. Kubicek. EpiSimS: Epidemic simulation system. Technical Report LAUR–06-6714, Los Alamos National Laboratory, 2006.
- [12] O. Diekmann, J. A. P. Heesterbeek, and J. A. J. Metz. On the definition and the computation of the basic reproduction ratio \mathcal{R}_0 in models for infectious diseases in heterogeneous populations. *Journal of Mathematical Biology*, 28:365–382, 1990.
- [13] S. N. Dorogovtsev, J. F. F. Mendes, and A. N. Samukhin. Giant strongly connected component of directed networks. *Physical Review E*, 64(2):025101, Jul 2001.
- [14] K. T. D. Eames. Modelling disease spread through random and regular contacts in clustered populations. *Theoretical Population Biology*, 73:104–111, 2008.
- [15] Stephen Eubank, Hasan Guclu, V S Anil Kumar, Madhav V Marathe, Aravind Srinivasan, Zoltán Toroczkai, and Nan Wang. Modelling disease outbreaks in realistic urban social networks. *Nature*, 429(6988):180–184, 2004.
- [16] Scott L. Feld. Why your friends have more friends than you do. *American Journal of Sociology*, 96(6):1464–1477, 1991.
- [17] Neil M. Ferguson, Derek A. T. Cummings, Simon Cauchemez, Christophe Fraser, Steven Riley, Aronrag Meeyai, Sophon Iamsirithaworn, and Donald S. Burke. Strategies for containing an emerging influenza pandemic in Southeast Asia. *Nature*, 437(7056):209–214, 2005.
- [18] W. Floyd, L. Kay, and M. Shapiro. Some elementary properties of SIR networks or, can I get sick because you got vaccinated? *Bulletin of Mathematical Biology*, 70(3):713–727, 2008.
- [19] Timothy C. Germann, Kai Kadau, Ira M. Longini Jr., and Catherine A. Macken. Mitigation strategies for pandemic influenza in the United States. *Proceedings of the National Academy of Sciences of the United States of America*, 103(15):5935–5940, 2006.
- [20] M. B. Hastings. Systematic series expansions for processes on networks. *Physical Review Letters*, 96(14):148701, 2006.
- [21] M. J. Keeling. The effects of local spatial structure on epidemiological invasions. *Proceedings of the Royal Society B: Biological Sciences*, 266(1421):859–867, 1999.
- [22] Eben Kenah and James M. Robins. Network-based analysis of stochastic SIR epidemic models with random and proportionate mixing. *Journal of Theoretical Biology*, 2007.
- [23] Eben Kenah and James M. Robins. Second look at the spread of epidemics on networks. *Physical Review E*, 76(3):36113, 2007.
- [24] W. O. Kermack and A. G. McKendrick. A contribution to the mathematical theory of epidemics. *Royal Society of London Proceedings Series A*, 115:700–721, August 1927.

- [25] Kari Kuulasmaa. The spatial general epidemic and locally dependent random graphs. *Journal of Applied Probability*, 19(4):745–758, 1982.
- [26] D. Ludwig. Final size distributions for epidemics. *Mathematical Biosciences*, 23:33–46, 1975.
- [27] Junling J. Ma and David J. D. Earn. Generality of the final size formula for an epidemic of a newly invading infectious disease. *Bulletin of Mathematical Biology*, 68(3):679–702, 2006.
- [28] M. Marder. Dynamics of epidemics on random networks. *Physical Review E*, 75(6):066103, 2007.
- [29] Lauren Ancel Meyers. Contact network epidemiology: Bond percolation applied to infectious disease prediction and control. *Bulletin of the American Mathematical Society*, 44(1):63–86, 2007.
- [30] Lauren Ancel Meyers, Mark Newman, and B. Pourbohloul. Predicting epidemics on directed contact networks. *Journal of Theoretical Biology*, 240(3):400–418, June 2006.
- [31] Lauren Ancel Meyers, Babak Pourbohloul, Mark E. J. Newman, Danuta M. Skowronski, and Robert C. Brunham. Network theory and SARS: predicting outbreak diversity. *Journal of Theoretical Biology*, 232(1):71–81, January 2005.
- [32] Joel C. Miller. Epidemic size and probability in populations with heterogeneous infectivity and susceptibility. *Physical Review E*, 76(1):010101, 2007.
- [33] Joel C. Miller. Bounding the size and probability of epidemics on networks. *Journal of Applied Probability*, 45:498–512, 2008.
- [34] M. Molloy and Bruce Reed. A critical point for random graphs with a given degree sequence. *Random structures & algorithms*, 6(2):161–179, 1995.
- [35] Joël Mossong, Niel Hens, Mark Jit, Philippe Beutels, Kari Auranen, Rafael Mikolajczyk, Marco Massari, Stefania Salmaso, Gianpaolo Scalia Tomba, Jacco Wallinga, Janneke Heijne, Malgorzata Sadkowska-Todys, Magdalena Rosinska, and W. John Edmunds. Social contacts and mixing patterns relevant to the spread of infectious diseases. *PLoS Medicine*, 5(3):381–391, 2008.
- [36] Mark E. J. Newman. Spread of epidemic disease on networks. *Physical Review E*, 66(1):16128, 2002.
- [37] Mark E. J. Newman. Properties of highly clustered networks. *Physical Review E*, 68(2):026121, 2003.
- [38] Mark E. J. Newman. The structure and function of complex networks. *SIAM Review*, 45:167–256, 2003.
- [39] Pierre-André Noël, Bahman Davoudi, Luis J. Dubé, Robert C. Brunham, and Babak Pourbohloul. Time evolution of disease spread on finite-size networks with degree heterogeneity. *Submitted*, 2008.
- [40] M. Ángeles Serrano and Marián Boguñá. Clustering in complex networks. II. Percolation properties. *Physical Review E*, 74(5):056115, 2006.
- [41] M. Ángeles Serrano and Marián Boguñá. Percolation and epidemic thresholds in clustered networks. *Physical Review Letters*, 97(8):088701, 2006.
- [42] Pieter Trapman. On analytical approaches to epidemics on networks. *Theoretical Population Biology*, 71(2):160–173, 2007.
- [43] DJ Watts and SH Strogatz. Collective dynamics of ‘small-world’ networks. *Nature*, 393(6684):409–410, 1998.